

## Multiple Scattering of Polarized Light in Planetary Atmospheres. Part II. Sunlight Reflected by Terrestrial Water Clouds

JAMES E. HANSEN

*Goddard Institute for Space Studies, NASA, New York, N. Y.*

(Manuscript received 3 August 1971, in revised form 23 August 1971)

### ABSTRACT

The intensity and polarization of sunlight reflected by terrestrial water clouds are computed with the doubling method. The calculations illustrate that this method can be effectively used in problems involving strongly anisotropic phase matrices. The method can therefore be used to derive information about planetary clouds, including those of the earth, from polarimetric observations.

The results of the computations indicate that the polarization is more sensitive than the intensity to cloud microstructure, such as the particle size and shape. Multiple scattering does not wash out features in the polarization as effectively as it does in the intensity, because the polarization arises primarily from photons scattered once or a small number of times. Hence polarization measurements, particularly in the near infrared, are potentially a valuable tool for cloud identification and for studies of the microphysics of clouds.

The computations are made primarily at four wavelengths in the near infrared, from 1.2 to 3.4  $\mu$ . The results for  $\lambda = 1.2 \mu$  are also applicable to scattering at visual and ultraviolet wavelengths. The other wavelengths are selected to illustrate the basic scattering characteristics in the near infrared for reflection of sunlight from water clouds.

It is shown that the intensity computed with the exact theory including polarization differs by  $\lesssim 1.0\%$  from the intensity computed in the common scalar approximation in which the polarization is neglected. Therefore, when only the intensity is required, and not the polarization, it is possible in most cases to neglect polarization entirely.

An approximation obtained by setting the phase matrix elements  $P^{34}(\alpha)$  and  $P^{43}(\alpha)$  equal to zero is proposed and tested. It is found that this introduces errors less than one part in  $10^6$  for the intensity and errors  $\lesssim 0.0002$  in the degree of polarization. This means that in computing the polarization properties for multiple scattering by spherical particles it is usually adequate to work with 3 by 3 matrices.

An examination is made of the accuracy of the polarization in the approximation in which it is assumed that multiply scattered photons are unpolarized. A modified version of this, which, in addition, takes advantage of the fact that diffracted light is nearly unpolarized, is also tested. The modified approximation is found to yield an improved accuracy in most cases.

Another approximation, which can be termed a renormalization method, is described and tested. The method consists of modifying the phase matrix for single scattering so that the integrations over zenith angle can be performed with a small number of points. The order of the approximation (the number of zenith angles in the integrations) can easily be varied and accuracies sufficient for practical applications can be obtained at low orders of approximation. The method is therefore useful for small computers.

### 1. Introduction

The microphysics of clouds is generally assumed to be intimately connected with the general dynamic and thermodynamic processes in individual cloud bodies, as well as with the synoptics of entire weather systems. An improved understanding of the relations of the microphysics to the meso- and macrophysics is essential to the sciences of both weather prediction and weather modification.

Methods of remotely sensing cloud particle phase and size distribution are needed to help relate the microstructure to the cloud type. Furthermore, with an understanding of these relations in hand, it is possible that measurements from satellites of the microstructure

of clouds could be of significant value for weather prediction.

Active methods of remote sensing, for example with radar or lasers, can be used for investigating local cloud systems. However, to obtain information over a wide geographic area with a satellite-borne sensor, it is desirable to use reflected sunlight as the probe. It has already been shown (Blau *et al.*, 1966; Hovis and Tobin, 1967; Hansen and Pollack, 1970) that some information on the cloud microstructure can be obtained by observing the intensity of reflected sunlight in the near infrared. It is likely that the polarization of reflected sunlight is more sensitive than the intensity to cloud microstructure. This paper represents one step

in an attempt to determine how the polarization can best be employed in cloud studies.

## 2. Computational procedure

In preceding papers [Hansen, 1969a, 1971 (the latter<sup>1</sup> being referred to here as Part I)], we described the doubling method for computing the multiple scattering of light from a plane-parallel atmosphere. In this paper we illustrate that the method can be used for computations of the polarization of sunlight reflected by terrestrial water clouds.

### a. Wavelengths

The calculations are made for the near-infrared wavelength region, from  $\lambda = 1 \mu$  to  $\lambda = 3.5 \mu$ , because that region is the most promising for studies of cloud microstructure. First, the optical properties of water (and ice) undergo significant variations in this region; these variations can be exploited for establishing both the particle phase and size distribution. Second, the wavelength in this region is closer in value to the particle size than it is in the visual region; therefore, the scattering properties are more sensitive to the particle size in the infrared than at shorter wavelengths. The calculations in this paper are made for four wavelengths,  $\lambda = 1.2, 2.25, 3.1$  and  $3.4 \mu$ , which illustrate well the basic scattering properties of water clouds in the near infrared. In one figure the wavelengths 1.0 and  $3.5 \mu$  are also considered.

At  $\lambda = 1.2 \mu$  the size parameter  $x (= 2\pi r/\lambda) \gtrsim 25$  for typical cloud particles and the absorptivity of water is practically negligible; hence, features arising in geometrical optics from rays which travel within the sphere, e.g., the primary rainbow, are present. Thus, the scattering properties of water clouds would be similar for the range  $0.3 \mu \lesssim \lambda \lesssim 1.2 \mu$ , with the results for decreasing wavelength being closer to the limit of geometrical optics (Liou and Hansen, 1971).

At  $\lambda = 3.4 \mu$  the wavelength is about as close to the size of typical cloud particles as it is possible to go without encountering severe thermal emission from the clouds. The sensitivity of the scattering properties to the particle size are further enhanced at this wavelength by the absorptivity of water which is sufficient to significantly attenuate rays traveling within the particle; the attenuation, of course, increases with the particle size.

<sup>1</sup> Several papers not included in the discussion section of Part I have recently been published for cases more complicated than Rayleigh scattering. Hovenier (1971) describes the doubling method and presents calculations with an analytic haze model for the phase matrix. Herman *et al.* (1971) present calculations of the transmitted light for a hazy atmosphere using the computational method Herman developed earlier (Herman, 1965; Herman and Browning, 1965). Kattawar and Plass (1971) modify their Monte Carlo method so that it can be efficiently used for optically thick, as well as optically thin, atmospheres; they make computations for scattering by model terrestrial clouds.

At  $\lambda = 2.25 \mu$  both the size parameter and the absorptivity of water are intermediate between their values at  $1.2$  and  $3.4 \mu$ .

At  $\lambda = 3.1 \mu$  the absorptivity of water is so large that rays cannot penetrate the particle. Except for diffraction most of the scattered light is due to Fresnel reflection from the outside of the particles and it has a high degree of polarization.

All of these wavelengths fall in windows of the near IR gaseous absorption spectrum in the terrestrial atmosphere. This is important because it has been found (see, e.g., Hansen and Pollack, 1970) that  $\text{CO}_2$  and  $\text{H}_2\text{O}$  absorption cause considerable difficulty in attempts to interpret the near IR spectral and angular reflectivities of water clouds.

### b. Particle size distribution

Most of the computations in this paper are for the particle size distribution<sup>2</sup>

$$n(r) = \text{constant } r^{(1-3b)/b} e^{-[r/(ab)]}, \quad (1)$$

where  $n(r)dr$  is the number of particles per unit volume with radius between  $r$  and  $r+dr$ . This distribution is a variation of the gamma distribution (Kendall and Stuart, 1963); other forms of the gamma distribution have been used as models for cloud particle size distributions by Khrgian and Mazin (1952, 1956), Deirmendjian (1964), Hansen and Pollack (1970), and others (see, e.g., Khrgian, 1961). In the size distribution (1) the two parameters  $a$  and  $b$  have important physical meanings; they are equal to the *mean effective radius* and the *effective variance* for this size distribution.

We define the mean effective radius for any cloud particle size distribution as

$$\langle r \rangle_{\text{eff}} = \frac{\int_0^\infty r \pi r^2 n(r) dr}{\int_0^\infty \pi r^2 n(r) dr}. \quad (2)$$

This differs from the simple mean radius only in that we have included the particle area as a weight factor multiplying  $n(r)$ . This weight factor is included since a cloud particle scatters an amount of light approximately in proportion to its area. It is clear that the mean effective radius is a significant characterization of a cloud particle size distribution for describing the scattering properties of that distribution.<sup>3</sup> Indeed, for some properties of the scattered light  $\langle r \rangle_{\text{eff}}$  is an adequate characterization of the size distribution. However, higher moments can sometimes be important,

<sup>2</sup> If  $N = \int_0^\infty n(r) dr$  is the total number of particles per unit volume, then  $\text{constant} = N (ab)^{(2b-1)/b} / \Gamma[(1-2b)/b]$ . However, since we only need the normalized phase matrix in this paper, the value of the constant is not required here.

<sup>3</sup> See Appendix A for a more general discussion.

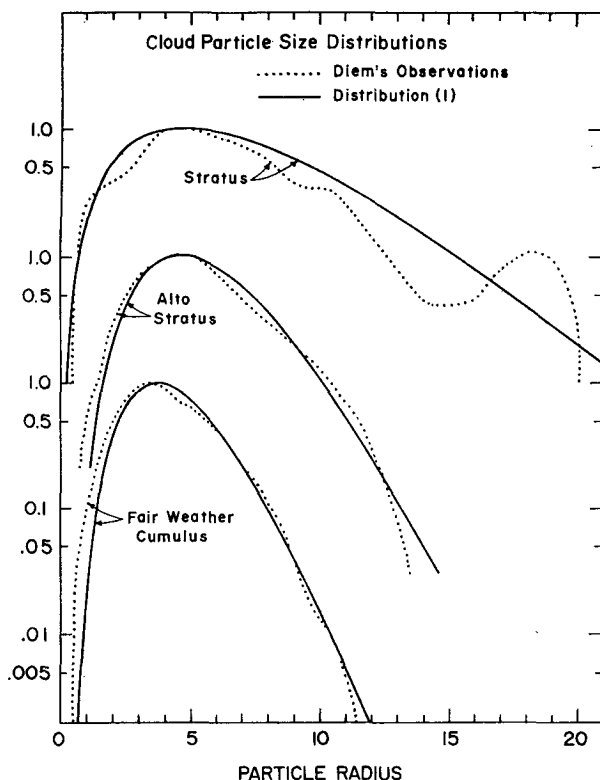


FIG. 1. Comparison of measured cloud particle size distributions (Diem, 1948) to the standard size distribution (1). The curves for the distribution (1) were obtained using  $a$  and  $b$  equal to  $\langle r \rangle_{\text{eff}}$  and  $v_{\text{eff}}$  in Table 1. All of the curves are normalized to unity at their maximum points, and each of the cloud types is successively displaced by an order of magnitude. The curves are thus proportional to  $n(r)$ . The radius is in microns.

particularly for polarization. We define the *effective variance* as

$$v_{\text{eff}} = \frac{\int_0^{\infty} (r - \langle r \rangle_{\text{eff}})^2 \pi r^2 n(r) dr}{\langle r \rangle_{\text{eff}}^2 \int_0^{\infty} \pi r^2 n(r) dr}, \quad (3)$$

where the factor  $\langle r \rangle_{\text{eff}}^2$  is included in the denominator to make  $v_{\text{eff}}$  dimensionless and a relative measure. Additional moments of the size distribution may be defined analogously, but, as we will show, there is little need of them for our purposes.

TABLE 1. Mean effective radius and effective variance of the cloud particle size distributions of Diem.

Cloud type	$\langle r \rangle_{\text{eff}}$	$v_{\text{eff}}$
Fair weather cumulus	5.56	0.111
Altostratus	7.01	0.113
Stratus	11.19	0.193
Cumulus congestus	10.48	0.147
Stratocumulus	5.33	0.118
Nimbostratus	10.81	0.143

Different cloud particle size distributions having the same values of  $\langle r \rangle_{\text{eff}}$  and  $v_{\text{eff}}$  will have similar scattering properties. In particular, an observed particle size distribution will have scattering properties similar to those of an analytic size distribution if we make sure that the observed and model distributions have the same values of  $\langle r \rangle_{\text{eff}}$  and  $v_{\text{eff}}$ . This is particularly easy to do for the distribution (1), because, as may be verified by substitution into (2) and (3),

$$\left. \begin{aligned} a &= \langle r \rangle_{\text{eff}} \\ b &= v_{\text{eff}} \end{aligned} \right\} \text{for the size distribution (1).}$$

Because the parameters  $a$  and  $b$  in (1) are equal to physical parameters which can characterize the scattering by the size distribution, we use (1) as a standard distribution for cloud particles.

Fig. 1 shows three cloud particle size distributions measured by Diem (1948). They are presented here only as examples of observed distributions, with no claims as to the reliability of the observations or the generality of the classification into cloud types. The three cloud types presented include the extremes observed by Diem: the narrowest (i.e., smallest  $v_{\text{eff}}$ ; fair weather cumulus and altostratus), the broadest (stratus), and the most strongly bimodal distribution (stratus). The fair weather cumulus distribution also has a mean effective radius close to the smallest of the distributions reported by Diem, and the stratus distribution has the largest  $\langle r \rangle_{\text{eff}}$ .

The values  $\langle r \rangle_{\text{eff}}$  and  $v_{\text{eff}}$  were computed for the observed distribution using (2) and (3). The results are shown in Table 1 which includes the results for the other cloud types reported by Diem. The corresponding standard size distributions, obtained from (1) with  $a = \langle r \rangle_{\text{eff}}$  and  $b = v_{\text{eff}}$ , are also plotted in Fig. 1.

In Fig. 2 we have plotted the phase function and degree of polarization for single scattering by both the observed size distributions and the corresponding standard distributions. In the calculations for this figure the integrations over particle size were made from  $r_1 = 0$  to  $r_2 = 21 \mu$ . That this cutoff did not significantly affect the phase functions and polarizations was verified by calculations with  $r_2 = 30 \mu$ . Single scattering is discussed in greater detail in Section 3; we note here only that the observed and standard size distributions have remarkably similar scattering properties. Comparable results were obtained at intermediate and shorter wavelengths and for other observed cloud particle size distributions. The differences which do exist are larger for the polarization than the intensity, and they are usually greatest in the region between the rainbow and the glory.

In this paper some multiple scattering calculations are made with observed cloud particle size distributions (Section 4d). However, most of the calculations are for the standard distribution (1) with  $a = 6 \mu$  and  $b = \frac{1}{3}$ . In

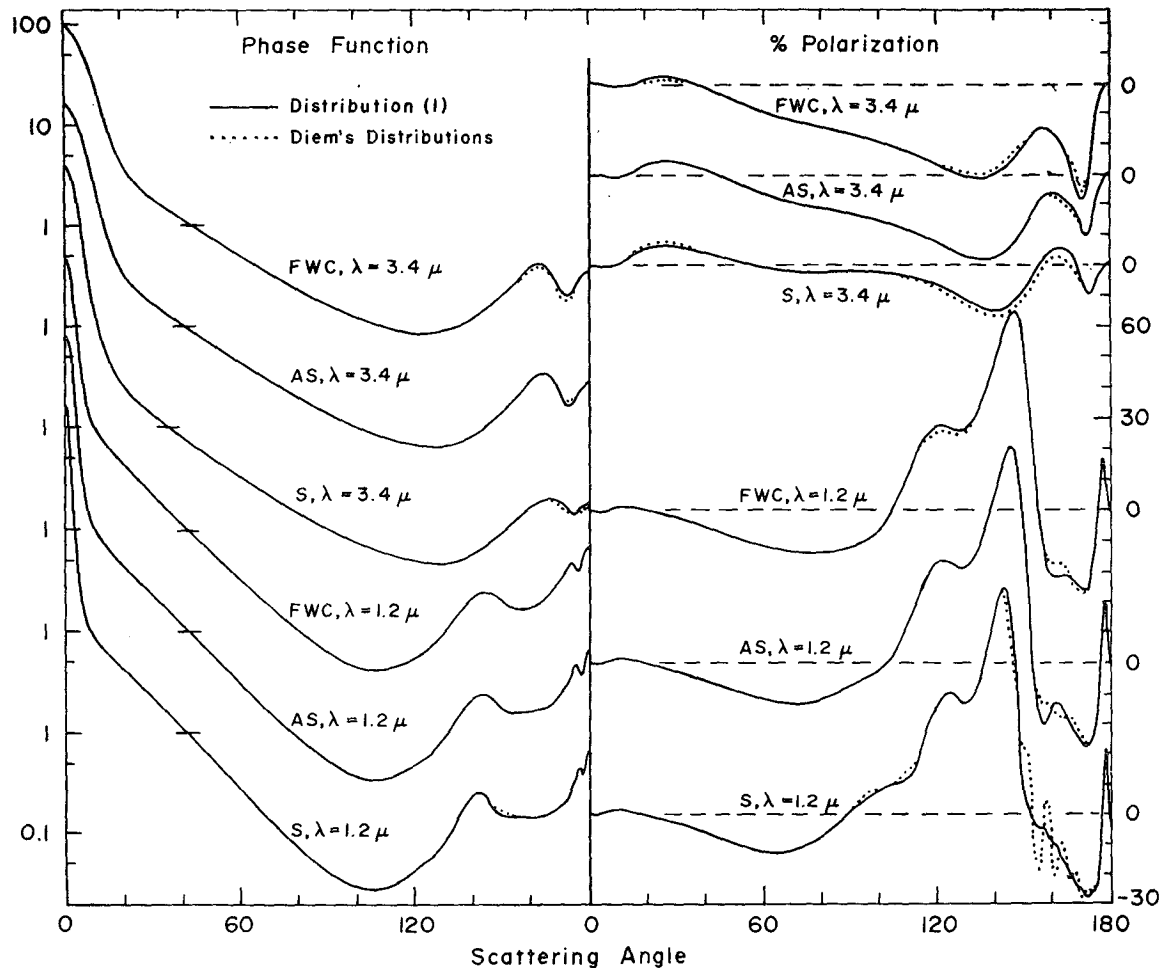


FIG. 2. Phase function ( $P^{11}$ ) and percent polarization ( $-100P^{21}/P^{11}$ ) for single scattering by spherical particles for the size distributions in Fig. 1. FWC, AS and S represent fair weather cumulus, altostratus and stratus, respectively. The phase functions are successively displaced from one another by an order of magnitude with the horizontal bars occurring at the value unity. The polarizations are displaced from one another with the dashed lines indicating zero polarization.

this case the distribution is identical to the cloud model for which Deirmendjian (1964) made single scattering computations; this model has been used extensively in the literature and represents reasonably well the fair weather cumulus clouds observed by Diem (1948) and Durbin (1959). It should be emphasized, though, that the values  $a=6\mu$  and  $b=\frac{1}{3}$  are only representative of some cloud types, at some points in the clouds, and then only when the average over several samples is taken. Cloud particle size distributions are known to vary with time (Squires, 1958; Okita, 1961; Ludwig and Robinson, 1971) and with height and horizontal location in the cloud (Zaitsev, 1950; Weickmann and aufm Kampe, 1953; Squires, 1958; Warner, 1969). Characteristic differences in the size distributions of the various cloud types do exist, however, and some information is available on the change in the size distribution which occurs with the development of clouds, e.g., during the transition from a non-raining to a raining state. The question of whether the variations of

the size distribution are sufficient to allow identification of the cloud type and detection of changes in the cloud state by means of the polarization of reflected sunlight is discussed in Section 6.

The primary purpose of this paper is to make calculations of the intensity and polarization of light multiply scattered by a realistic model of terrestrial clouds; this is sufficient to allow the effectiveness of the doubling method to be tested, to allow some general conclusions to be made about the effect of multiple scattering on the polarization of light reflected by clouds, and to allow the testing of some approximations for multiple scattering. We also make a limited investigation of the effect of particle size on the scattered light by making calculations with  $a=3, 6, 12$  and  $24\mu$ . We use this large range because some observers (e.g., Weickmann and aufm Kampe, 1953; Squires, 1958) have reported cloud particle size distributions with mean effective radii much larger than those for the distributions reported by Diem (1948). In this paper we do not specifically

TABLE 2. Single-scattering albedo,  $\tilde{\omega}_0$ , and asymmetry parameter,  $\langle \cos \alpha \rangle$ , for the size distribution (1) with  $b = \frac{1}{3}$ .

		Wavelength			
		$\lambda = 1.2 \mu$	$\lambda = 2.5 \mu$	$\lambda = 3.1 \mu$	$\lambda = 3.4 \mu$
$\tilde{\omega}_0$	$n_r$	1.323	1.290	1.426	1.449
	$n_i$	$9.74 \times 10^{-6}$	$3.04 \times 10^{-4}$	0.1828	0.01888
	$a = 3 \mu$	0.999706	0.996541	0.5148	0.8661
	$a = 6 \mu$	0.999379	0.990757	0.4909	0.7285
	$a = 12 \mu$	0.998818	0.981374	0.5115	0.6289
$\langle \cos \alpha \rangle$	$a = 24 \mu$	0.998038	0.969260	0.5264	0.5668
	$a = 3 \mu$	0.7804	0.8412	0.8843	0.7659
	$a = 6 \mu$	0.8311	0.8016	0.9308	0.7910
	$a = 12 \mu$	0.8550	0.8495	0.9479	0.8898
	$a = 24 \mu$	0.8677	0.8720	0.9523	0.9336

investigate the effect of  $b$  on the scattered light, which is clearly secondary to the effect of  $a$ .

The calculations here are for a homogeneous atmosphere; thus, the size distribution is taken as being constant with height in the cloud. This simplification should not lead to serious difficulty in interpreting the polarization, however. The polarization arises primarily from the particles in the very tops of the clouds (see Section 5c), and hence the properties assumed for the homogeneous atmosphere may be taken as corresponding to those in the cloud top. Variations in cloud properties at greater depths would primarily affect the intensity of the reflected light, which in turn affects the degree of polarization in a simple manner.

### 3. Single scattering

The doubling method may be applied after the phase matrix  $\mathbf{P}(\alpha)$  and single scattering albedo  $\tilde{\omega}_0$  have been determined (Hansen, 1969a, 1971). These may be obtained for homogeneous isotropic spheres from the well-known Mie theory (van de Hulst, 1957). The phase matrix for such a single sphere may be described, in the notation of van de Hulst, by four functions of the radius and scattering angle,  $M_1(r, \alpha)$ ,  $M_2(r, \alpha)$ ,  $S_{21}(r, \alpha)$  and  $D_{21}(r, \alpha)$ . In the case of a size distribution of particles, which are assumed to scatter independently, the corresponding functions are obtained by integrating over all particles in the size distribution, e.g.,

$$M_1(\alpha) = \int_{r_1}^{r_2} M_1(r, \alpha) n(r) dr. \quad (4)$$

The phase matrix for homogeneous isotropic spheres then has the form

$$\mathbf{P}(\alpha) = \begin{pmatrix} P^{11} & P^{21} & 0 & 0 \\ P^{21} & P^{22} & 0 & 0 \\ 0 & 0 & P^{33} & -P^{43} \\ 0 & 0 & P^{43} & P^{33} \end{pmatrix}, \quad (5)$$

where

$$\left. \begin{aligned} P^{11}(\alpha) &= c[M_2(\alpha) + M_1(\alpha)]/2 \\ P^{21}(\alpha) &= c[M_2(\alpha) - M_1(\alpha)]/2 \\ P^{33}(\alpha) &= cS_{21}(\alpha) \\ P^{43}(\alpha) &= cD_{21}(\alpha) \end{aligned} \right\} \quad (6)$$

and  $c$  is a constant defined such that the phase function  $P^{11}(\alpha)$  is normalized as

$$\frac{1}{4\pi} \int_{4\pi} P^{11}(\alpha) d\omega = 1. \quad (7)$$

The phase function  $P^{11}(\alpha)$  represents the "gain" with respect to isotropic scattering, i.e., for isotropic scattering  $P^{11}(\alpha) = 1$ .

More details of the theory for single scattering by spheres are given by van de Hulst (1957) and Deirmendjian (1969). The single scattering depends on the size distribution of spheres,  $n(r)$ , and the optical constants  $n_r$  and  $n_i$ , the real and imaginary parts of the refractive index of the spheres. Table 2 gives the optical constants of water, taken from Irvine and Pollack (1968), at  $\lambda = 1.2, 2.25, 3.1$  and  $3.4 \mu$ . Also given in Table 2 are the values of the single scattering albedo  $\tilde{\omega}_0$  and the asymmetry parameter of the phase function,

$$\langle \cos \alpha \rangle = \frac{1}{4\pi} \int_{4\pi} \cos \alpha P^{11}(\alpha) d\omega, \quad (8)$$

both computed for the size distribution (1) with  $b = \frac{1}{3}$ . The integrations over particle size were made from  $r_1 = 0$  to  $r_2 = 30 \mu$ . The terms  $\tilde{\omega}_0$  and  $\langle \cos \alpha \rangle$  are useful characterizations of the phase function (and the phase matrix); they are required, along with the optical thickness  $\tau$ , in many approximate treatments of multiple scattering.

Table 3 gives the phase matrix at  $\lambda = 2.25 \mu$  for the size distribution (1) with  $a = 6 \mu$  and  $b = \frac{1}{3}$ . The integrations over particle size were made from  $r_1 = 0$  to  $r_2 = 30 \mu$ . The numbers in Table 3 are expected to be accurate to the number of digits given, as indicated by the results of varying the number of points in the integration over size. The purpose of giving Table 3 is to allow other programs or computing methods for multiple scattering to be checked against our results, particularly for Section 5d. The phase matrix for  $\lambda = 2.25 \mu$  is used since it is sufficiently smooth to provide a tractable problem for moderate-sized computers, and yet it has characteristic cloud features such as the rainbow, glory and diffraction peak.

Figs. 3-6 show the phase function and percent polarization for single scattering at  $\lambda = 1.2, 2.25, 3.1$  and  $3.4 \mu$ . The percent polarization for single scattering is defined here as  $-100(P^{21}/P^{11})$ . The results are for the size distribution (1) with  $b = \frac{1}{3}$  and  $a = 3, 6, 12$  and  $24 \mu$ ; thus, the effective variance is not changed, but the effective mean radius is varied over a wide range.

TABLE 3. Phase matrix at  $\lambda = 2.25 \mu$  for size distribution (1) with  $a = 6 \mu$  and  $b = \frac{1}{9}$ .

$\alpha$	$M_2$	$M_1$	$S_{21}$	$D_{21}$	$\alpha$	$M_2$	$M_1$	$S_{21}$	$D_{21}$
0.0	1.854 +2	1.854 +2	1.854 +2	0.0	92.0	9.319 -2	6.748 -2	4.819 -2	-2.439 -2
0.2	1.851 +2	1.851 +2	1.851 +2	7.638 -3	94.0	8.801 -2	6.378 -2	4.370 -2	-2.440 -2
0.4	1.843 +2	1.843 +2	1.843 +2	3.041 -2	96.0	8.365 -2	6.088 -2	3.992 -2	-2.463 -2
0.6	1.830 +2	1.829 +2	1.829 +2	6.790 -2	98.0	8.006 -2	5.878 -2	3.676 -2	-2.513 -2
0.8	1.811 +2	1.810 +2	1.811 +2	1.194 -1	100.0	7.719 -2	5.749 -2	3.417 -2	-2.592 -2
1.0	1.787 +2	1.786 +2	1.786 +2	1.840 -1	102.0	7.500 -2	5.700 -2	3.206 -2	-2.708 -2
1.2	1.758 +2	1.757 +2	1.758 +2	2.605 -1	104.0	7.348 -2	5.733 -2	3.039 -2	-2.864 -2
1.4	1.725 +2	1.724 +2	1.724 +2	3.476 -1	106.0	7.263 -2	5.851 -2	2.909 -2	-3.067 -2
1.6	1.687 +2	1.686 +2	1.687 +2	4.437 -1	108.0	7.246 -2	6.054 -2	2.812 -2	-3.324 -2
1.8	1.646 +2	1.644 +2	1.645 +2	5.471 -1	110.0	7.301 -2	6.348 -2	2.743 -2	-3.641 -2
2.0	1.601 +2	1.599 +2	1.600 +2	6.562 -1	112.0	7.430 -2	6.738 -2	2.700 -2	-4.029 -2
2.5	1.477 +2	1.474 +2	1.475 +2	9.414 -1	114.0	7.639 -2	7.234 -2	2.683 -2	-4.495 -2
3.0	1.340 +2	1.336 +2	1.338 +2	1.223 +0	116.0	7.931 -2	7.847 -2	2.691 -2	-5.049 -2
3.5	1.197 +2	1.193 +2	1.195 +2	1.475 +0	118.0	8.307 -2	8.595 -2	2.727 -2	-5.702 -2
4.0	1.055 +2	1.050 +2	1.052 +2	1.679 +0	120.0	8.767 -2	9.495 -2	2.793 -2	-6.461 -2
4.5	9.176 +1	9.122 +1	9.140 +1	1.822 +0	122.0	9.302 -2	1.057 -1	2.895 -2	-7.334 -2
5.0	7.894 +1	7.836 +1	7.853 +1	1.900 +0	124.0	9.899 -2	1.186 -1	3.036 -2	-8.319 -2
6.0	5.691 +1	5.635 +1	5.647 +1	1.871 +0	126.0	1.053 -1	1.336 -1	3.222 -2	-9.408 -2
7.0	4.022 +1	3.973 +1	3.978 +1	1.655 +0	128.0	1.116 -1	1.511 -1	3.459 -2	-1.058 -1
8.0	2.841 +1	2.804 +1	2.803 +1	1.347 +0	130.0	1.174 -1	1.710 -1	3.751 -2	-1.178 -1
9.0	2.048 +1	2.023 +1	2.017 +1	1.027 +0	132.0	1.220 -1	1.931 -1	4.103 -2	-1.295 -1
10.0	1.532 +1	1.518 +1	1.509 +1	7.465 +1	134.0	1.248 -1	2.167 -1	4.518 -2	-1.400 -1
12.0	9.862 +0	9.868 +0	9.757 +0	3.575 -1	136.0	1.251 -1	2.410 -1	4.997 -2	-1.480 -1
14.0	7.435 +0	7.499 +0	7.380 +0	1.527 -1	138.0	1.225 -1	2.644 -1	5.538 -2	-1.524 -1
16.0	6.118 +0	6.186 +0	6.074 +0	4.876 -2	140.0	1.169 -1	2.851 -1	6.132 -2	-1.518 -1
18.0	5.238 +0	5.282 +0	5.190 +0	-5.726 -3	142.0	1.089 -1	3.009 -1	6.765 -2	-1.452 -1
20.0	4.565 +0	4.574 +0	4.507 +0	-3.592 -2	144.0	9.978 -2	3.098 -1	7.410 -2	-1.325 -1
22.0	4.015 +0	3.986 +0	3.943 +0	-5.398 -2	146.0	9.158 -2	3.101 -1	8.030 -2	-1.142 -1
24.0	3.547 +0	3.483 +0	3.461 +0	-6.529 -2	148.0	8.679 -2	3.012 -1	8.580 -2	-9.218 -2
26.0	3.140 +0	3.047 +0	3.042 +0	-7.215 -2	150.0	8.787 -2	2.839 -1	9.008 -2	-6.909 -2
28.0	2.782 +0	2.665 +0	2.673 +0	-7.582 -2	152.0	9.670 -2	2.603 -1	9.274 -2	-4.831 -2
30.0	2.464 +0	2.329 +0	2.348 +0	-7.718 -2	154.0	1.139 -1	2.338 -1	9.356 -2	-3.309 -2
32.0	2.182 +0	2.035 +0	2.061 +0	-7.690 -2	156.0	1.384 -1	2.084 -1	9.275 -2	-2.578 -2
34.0	1.932 +0	1.776 +0	1.807 +0	-7.549 -2	158.0	1.679 -1	1.882 -1	9.096 -2	-2.728 -2
36.0	1.709 +0	1.550 +0	1.584 +0	-7.334 -2	160.0	1.993 -1	1.765 -1	8.952 -2	-3.687 -2
38.0	1.512 +0	1.353 +0	1.387 +0	-7.072 -2	162.0	2.313 -1	1.768 -1	9.145 -2	-5.316 -2
40.0	1.337 +0	1.181 +0	1.214 +0	-6.785 -2	164.0	2.694 -1	1.942 -1	1.036 -1	-7.686 -2
42.0	1.183 +0	1.031 +0	1.063 +0	-6.486 -2	166.0	3.288 -1	2.351 -1	1.364 -1	-1.118 -1
44.0	1.047 +0	9.005 -1	9.301 -1	-6.184 -2	168.0	4.193 -1	2.974 -1	1.929 -1	-1.515 -1
46.0	9.269 -1	7.875 -1	8.142 -1	-5.887 -2	170.0	5.023 -1	3.513 -1	2.519 -1	-1.535 -1
48.0	8.213 -1	6.894 -1	7.130 -1	-5.599 -2	171.0	5.098 -1	3.586 -1	2.665 -1	-1.202 -1
50.0	7.284 -1	6.044 -1	6.247 -1	-5.322 -2	172.0	4.787 -1	3.471 -1	2.597 -1	-6.019 -2
52.0	6.467 -1	5.306 -1	5.477 -1	-5.058 -2	173.0	4.107 -1	3.208 -1	2.221 -1	1.774 -2
54.0	5.748 -1	4.666 -1	4.805 -1	-4.808 -2	174.0	3.257 -1	2.929 -1	1.465 -1	9.469 -2
56.0	5.116 -1	4.111 -1	4.218 -1	-4.571 -2	175.0	2.599 -1	2.833 -1	3.091 -1	1.477 -1
58.0	4.561 -1	3.629 -1	3.706 -1	-4.349 -2	175.5	2.464 -1	2.914 -1	-4.008 -1	1.594 -1
60.0	4.072 -1	3.210 -1	3.259 -1	-4.140 -2	176.0	2.503 -1	3.098 -1	-1.175 -1	1.598 -1
62.0	3.641 -1	2.846 -1	2.868 -1	-3.946 -2	176.5	2.727 -1	3.387 -1	-1.987 -1	1.492 -1
64.0	3.262 -1	2.529 -1	2.527 -1	-3.764 -2	177.0	3.122 -1	3.764 -1	-2.804 -1	1.293 -1
66.0	2.928 -1	2.253 -1	2.228 -1	-3.596 -2	177.5	3.647 -1	4.201 -1	-3.588 -1	1.028 -1
68.0	2.633 -1	2.013 -1	1.966 -1	-3.441 -2	178.0	4.237 -1	4.657 -1	-4.299 -1	7.337 -2
70.0	2.374 -1	1.803 -1	1.736 -1	-3.297 -2	178.2	4.474 -1	4.834 -1	-4.554 -1	6.162 -2
72.0	2.145 -1	1.619 -1	1.535 -1	-3.165 -2	178.4	4.704 -1	5.003 -1	-4.790 -1	5.028 -2
74.0	1.942 -1	1.458 -1	1.358 -1	-3.045 -2	178.6	4.922 -1	5.161 -1	-5.003 -1	3.960 -2
76.0	1.764 -1	1.318 -1	1.203 -1	-2.935 -2	178.8	5.123 -1	5.304 -1	-5.193 -1	2.981 -2
78.0	1.607 -1	1.194 -1	1.066 -1	-2.836 -2	179.0	5.301 -1	5.431 -1	-5.356 -1	2.114 -2
80.0	1.468 -1	1.086 -1	9.459 -2	-2.746 -2	179.2	5.453 -1	5.538 -1	-5.492 -1	1.376 -2
82.0	1.346 -1	9.916 -2	8.403 -2	-2.666 -2	179.4	5.575 -1	5.624 -1	-5.599 -1	7.839 -3
84.0	1.239 -1	9.087 -2	7.476 -2	-2.597 -2	179.6	5.665 -1	5.687 -1	-5.676 -1	3.517 -3
86.0	1.145 -1	8.364 -2	6.665 -2	-2.538 -2	179.8	5.720 -1	5.725 -1	-5.722 -1	8.840 -4
88.0	1.063 -1	7.737 -2	5.958 -2	-2.491 -2	180.0	5.738 -1	5.738 -1	-5.738 -1	0.0
90.0	9.927 -2	7.200 -2	5.346 -2	-2.457 -2					

The mode radii for these four size distributions are at 2, 4, 8 and 16  $\mu$ , respectively; the same distributions were used by Hansen and Pollack (1970) and the case  $a = 6 \mu$  is Deirmendjian's (1964) cloud model. The limits for the integration over particle size were the same as mentioned above for  $\bar{\omega}_0$  and  $\langle \cos \alpha \rangle$ .

Fig. 3 illustrates the single scattering results at  $\lambda = 1.2 \mu$  where the particles are essentially clear

(non-absorbing). These results are also approximately applicable for water at shorter wavelengths,  $0.3 \mu \leq \lambda' < 1.2 \mu$ , but the values indicated for  $a$  should be replaced by  $a' = (\lambda'/1.2 \mu)a$  for the results to apply at the shorter wavelengths. Both the features occurring in the phase function and the features in the polarization are potentially useful for establishing the size and phase of cloud particles from scattered sunlight; therefore, it is worth-

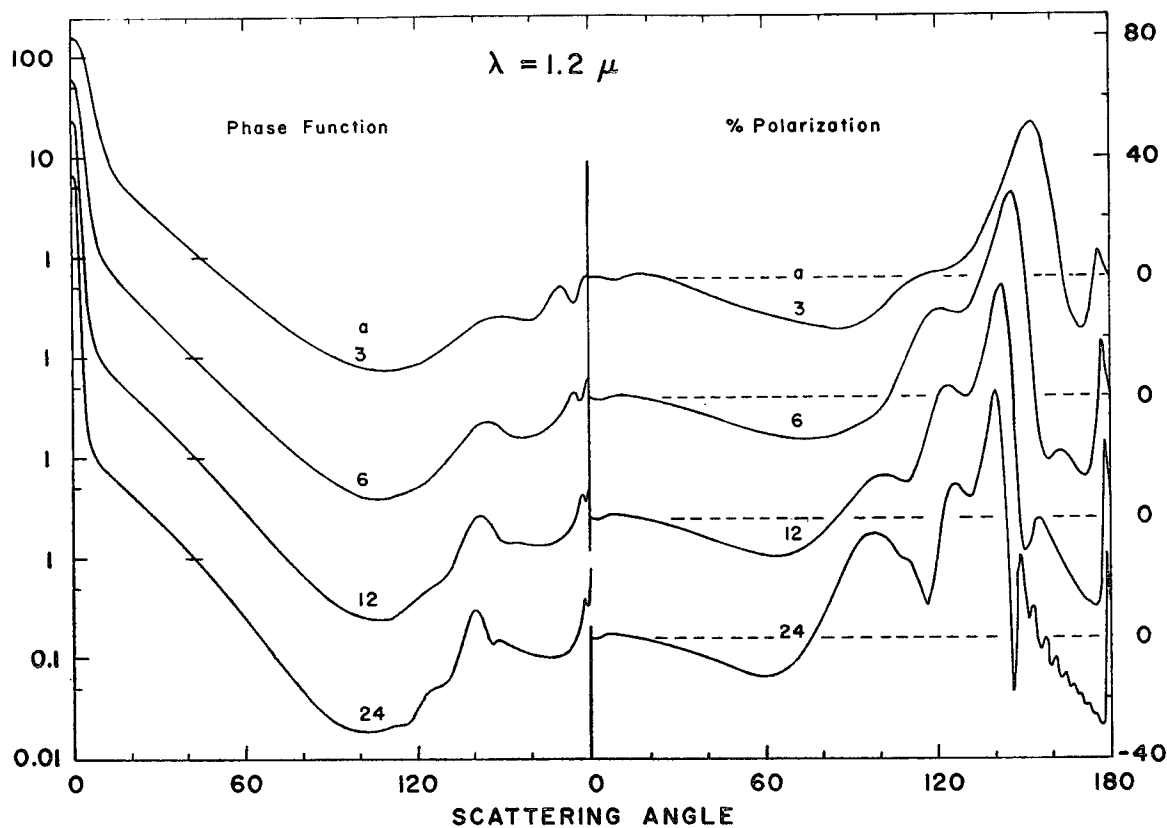


FIG. 3. Phase function ( $P^{11}$ ) and percent polarization ( $-100P^{21}/P^{11}$ ) for single scattering by spherical particles. The calculations are at  $\lambda = 1.2 \mu$  for the size distribution (1) with  $b = \frac{1}{3}$ . Results are shown for four values of  $a$  (in  $\mu$ ); for the distribution (1)  $a$  is equal to the effective radius for the distribution,  $\langle r \rangle_{\text{eff}}$ . The phase functions are successively displaced from one another, the dashed lines indicating zero polarization.

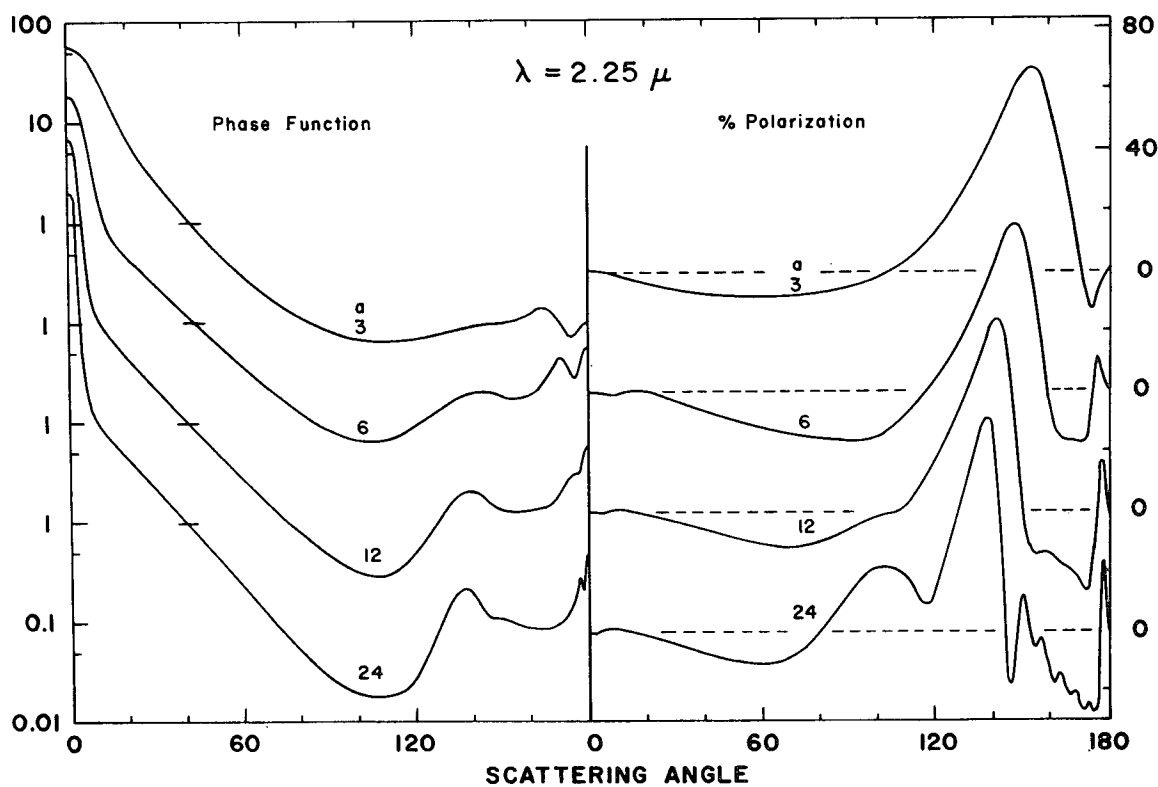
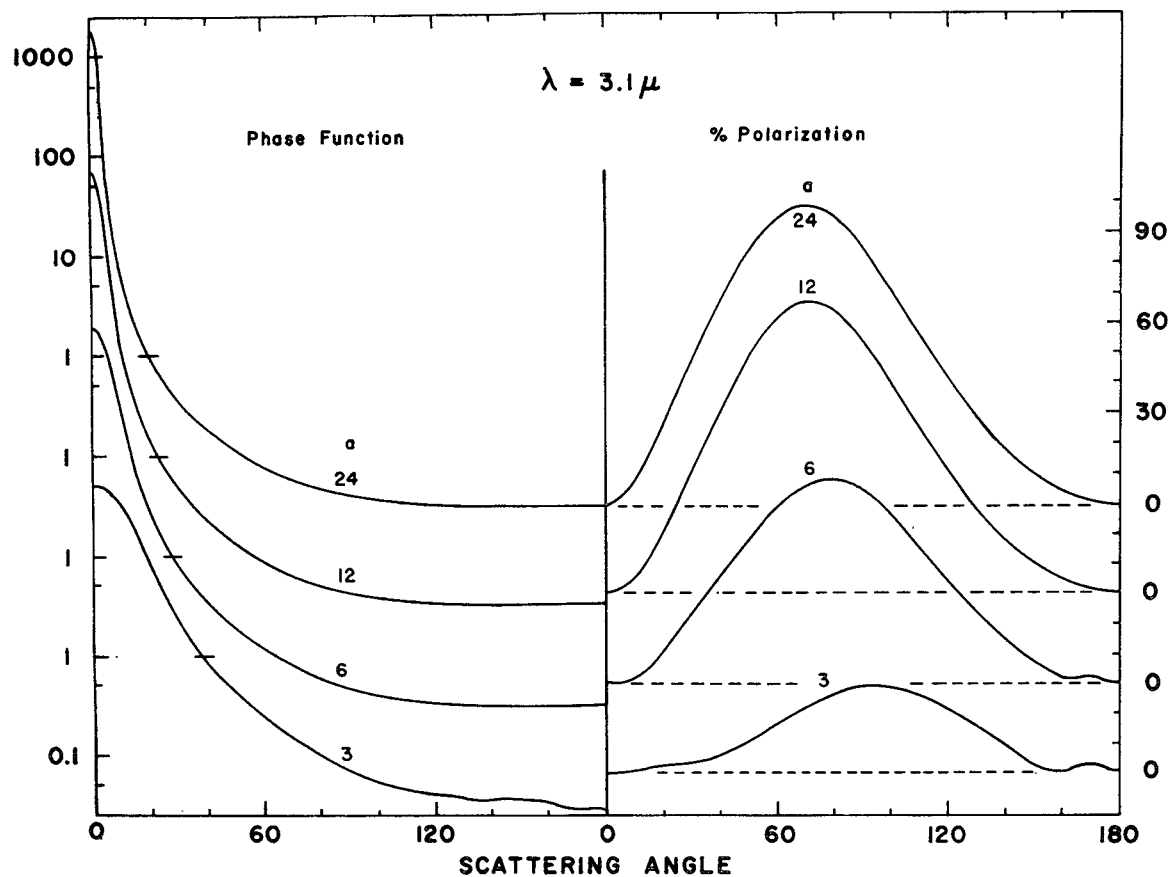
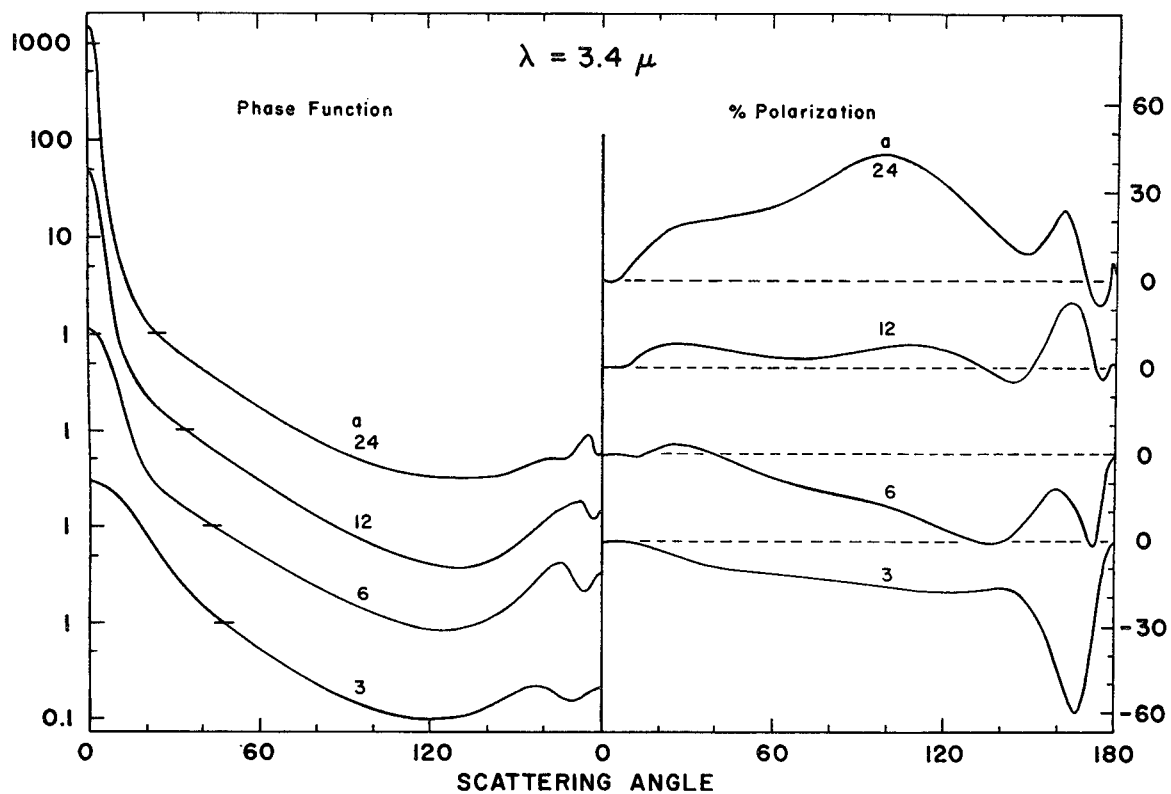


FIG. 4. Same as Fig. 3 except for  $\lambda = 2.25 \mu$ .

FIG. 5. Same as Fig. 3 except for  $\lambda = 3.1 \mu$ .FIG. 6. Same as Fig. 3 except for  $\lambda = 3.4 \mu$ .

while to compare the relative magnitude of these features in the phase function and polarization.

The strong diffraction peak in the phase function at  $\alpha \approx 0^\circ$  has no significant corresponding feature in the polarization, because diffracted light is essentially unpolarized. The magnitude and width of the diffraction peak depend on  $a$  in a simple manner, and hence could be useful for particle sizing. However, the diffraction peak occurs in reflected sunlight only if the sun is near the horizon.

The region of twice-refracted rays, from  $\alpha \approx 10^\circ$  to  $\alpha \approx 90^\circ$ , is characterized by primarily negative polarization and a decreasing intensity with increasing scattering angle. At this wavelength, which has no significant absorption, neither the phase function nor the polarization is strongly dependent on  $a$ , but the polarization is more sensitive than the phase function.

The *primary rainbow*, at  $\alpha \approx 140^\circ$ , arises from rays internally reflected once in spherical particles. The rainbow moves toward its position in geometrical optics (Liou and Hansen, 1971) and becomes increasingly sharp as  $a$  increases, in both the phase function and polarization. The polarization in the rainbow exceeds 80% for  $a = 24 \mu$ . The rainbow is more distinct in the polarization than in the phase function, particularly for the smaller values of  $a$ .

The *second rainbow* is the feature at scattering angles just smaller than those of the primary rainbow; it arises from rays twice internally reflected. The second rainbow is only noticeable in the phase function for  $a = 24 \mu$ , while it can be seen in the polarization for single scattering at all four values of  $a$ .

The *supernumerary bows* are interference maxima and minima which occur at scattering angles just larger than those of the primary rainbow. In the phase function only the first bow can be seen, and this only for  $a = 24 \mu$ . However, in the polarization for single scattering the first bow is apparent for both  $a = 6$  and  $12 \mu$ ; for  $a = 24 \mu$  a series of supernumerary bows are visible in the polarization with the first one being very strong.

*Fresnel reflection* from the outside of the particles leaves a feature of positive polarization in the single scattering for  $a = 12$  and  $24 \mu$  at  $\alpha \approx 100^\circ$ . There is no noticeable feature in the phase function due to Fresnel reflection.

The *glory* is the feature at  $\alpha \approx 180^\circ$ . This is clearly visible in both the phase function and the polarization for single scattering.

At  $\lambda = 2.25 \mu$  (Fig. 4) the features are analogous to those at  $\lambda = 1.2 \mu$ , the main difference being the smaller size parameter at  $\lambda = 2.25 \mu$ . The absorption in the particles at  $2.25 \mu$  is small, but it essentially removes the second rainbow. The absorption can also be expected to be much more effective in reducing multiple scattering than the absorption at  $\lambda = 1.2 \mu$ .

At  $\lambda = 3.1 \mu$  (Fig. 5) the absorption is so strong that essentially no rays can pass through the particles. Most

of the scattered light arises from diffraction, but this is unpolarized and concentrated in the forward direction. In other directions most of the scattered light is due to Fresnel reflection and is strongly polarized. The polarization is reminiscent of Rayleigh scattering, but the phase function is entirely different, the albedo for single scattering is low (Table 2) and the maximum in the polarization is not at  $\alpha = 90^\circ$ . For  $a \lesssim 12 \mu$  the polarization is sensitive to the particle size.

At  $\lambda = 3.4 \mu$  (Fig. 6) the polarization for single scattering is sensitive to the particle size at most scattering angles. This is partly because the absorption coefficient of water at this wavelength is such that the transmission of rays which are refracted into the sphere varies significantly with particle size. The sensitivity to particle size is also partly due to the fact that the wavelength and particle size are of the same order of magnitude, and hence the features of geometrical optics are disappearing for decreasing particle size.

From Figs. 3–6 it is clear that the phase function and particularly the polarization for single scattering contain information on the particle size. The single scattering also must depend on the particle shape, and therefore on the particle phase, because features such as the rainbows, the glory and the supernumerary bows arise because of the spherical shape of the particles (Liou and Hansen, 1971). For particles which differ significantly from the spherical shape these features in the single scattering would be lost, or at least greatly distorted. Our everyday experience confirms the absence of these features for ice clouds. Laboratory measurements of Lyot (1929) and Holland and Gagne (1970) also indicate that the rainbows are absent for irregular particles.

A major task is to examine how well the single scattering features survive the process of multiple scattering. This is considered in the following section.

#### 4. Multiple scattering

The reflection and transmission matrices,  $\mathbf{R}$  and  $\mathbf{T}$ , are obtained for a thin starting layer from the phase matrix as indicated by (20) and (21) in Part I. The reflection and transmission matrices for thicker layers are then obtained by repeated use of the doubling equations, (4)–(10) in Part I.

In this paper we present results only for the intensity and degree of polarization of the reflected light. The direction of polarization and the ellipticity of the reflected light can easily be obtained from the reflection matrix, but they are not essential for our purposes. All of the corresponding quantities describing the transmitted light can easily be obtained from the transmission matrix, but for clouds they are perhaps less interesting (because the polarization of the transmitted light is small) and in any case outside the scope of this paper.

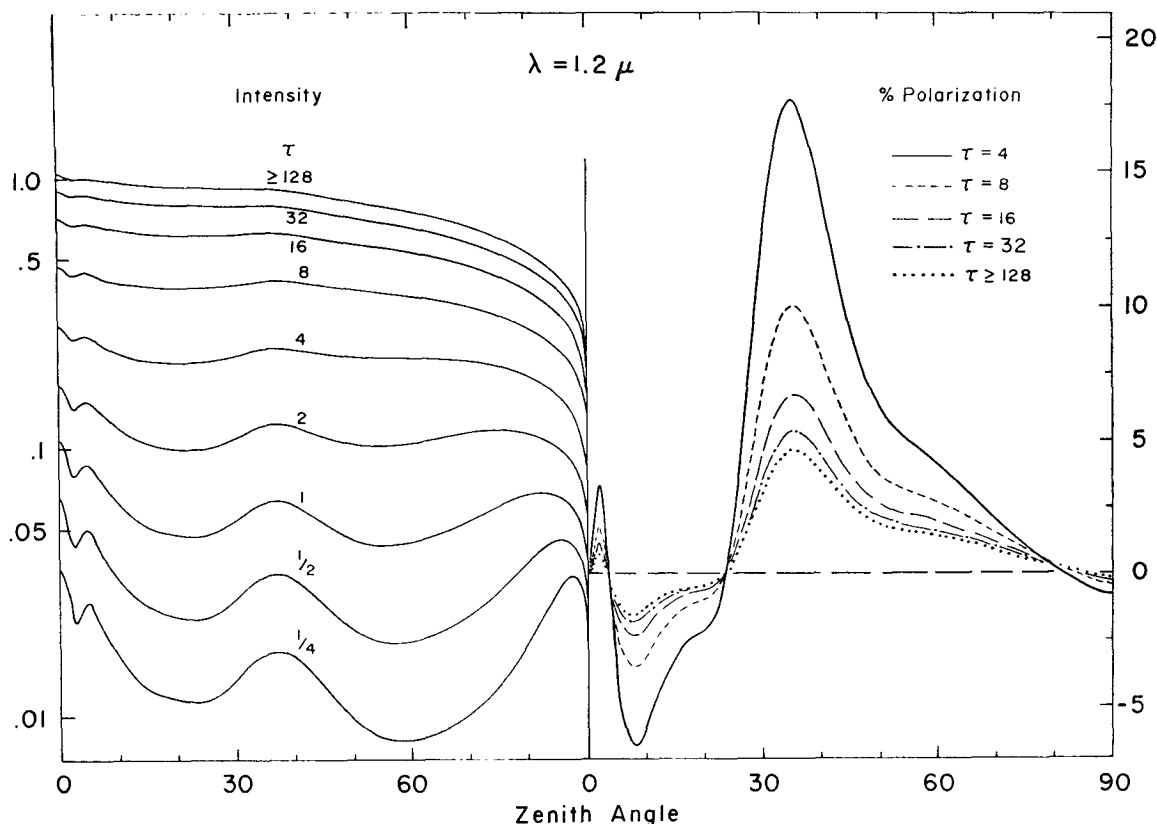


FIG. 7. Intensity ( $I = \mu_0 R^{11}$ ) and percent polarization ( $-100 Q/I = -100 R^{21}/R^{11}$ ) of sunlight reflected by a plane parallel cloud with the sun overhead ( $\theta_0 = 0^\circ$ ). The wavelength is  $1.2 \mu$  and results are shown for several optical thicknesses. On the horizontal axis is the zenith angle of the reflected light,  $\theta = \cos^{-1} \mu$ . The calculations are for the size distribution (1) with  $a = 6 \mu$  and  $b = \frac{1}{3}$ .

For the reflected intensity we have graphed

$$I = \mu_0 R^{11}.$$

To convert this to an absolute intensity (say, ergs  $\text{sec}^{-1} \text{cm}^{-2} \text{ster}^{-1} \mu^{-1}$ ) it must be multiplied by  $I_0/\pi$ , where  $I_0$  is the flux of the incident solar rays perpendicular to their direction; Allen (1963, p. 172), for example, gives a table of  $I_0$  (labeled  $f_\lambda$ ) for the solar spectrum.

The degree of polarization is

$$\frac{(Q^2 + U^2 + V^2)^{\frac{1}{2}}}{I},$$

which, for the unpolarized incident solar flux, is equal to

$$\frac{[(R^{21})^2 + (R^{31})^2 + (R^{41})^2]^{\frac{1}{2}}}{R^{11}}.$$

In the case of the sun at the zenith ( $\mu_0 = 1$ ),  $U = V = 0$  and hence we graph  $-Q/I$  as the degree of polarization. This contains more information than  $(Q^2)^{\frac{1}{2}}/I = |Q|/I$  because it illustrates the direction of polarization which (for  $\mu_0 = 1$ ) is either parallel or perpendicular to the plane of scattering, as indicated by the sign of  $-Q/I = (I_r - I_l)/I$ .

#### a. Normal incidence

The case of the sun at the zenith is commonly considered as a test case for computations of multiple scattering. This is a very special case since the results are azimuth-independent. The computational burden is greatly reduced in this special case; e.g., in the doubling method only the first term in the Fourier series expansions is nonzero. The computational simplifications may be the primary reason that this special case is often considered. However, it is also a practical case for the presentation of results since it allows them to be shown for all directions of scattering even when other parameters, such as the optical thickness, wavelength and particle size, are varied.

All of the figures (7-11) in this subsection are for the particle size distribution (1) with  $a = 6 \mu$  and  $b = \frac{1}{3}$ . The results in these, and in the other figures in this paper, are expected to be essentially exact, i.e., with any errors less than or on the order of the thickness of the curves. This was indicated by computational checks (obtained, e.g., by varying the number of integration points) and by checks against the results of other investigators (see, e.g., Hansen and Hovenier, 1971).

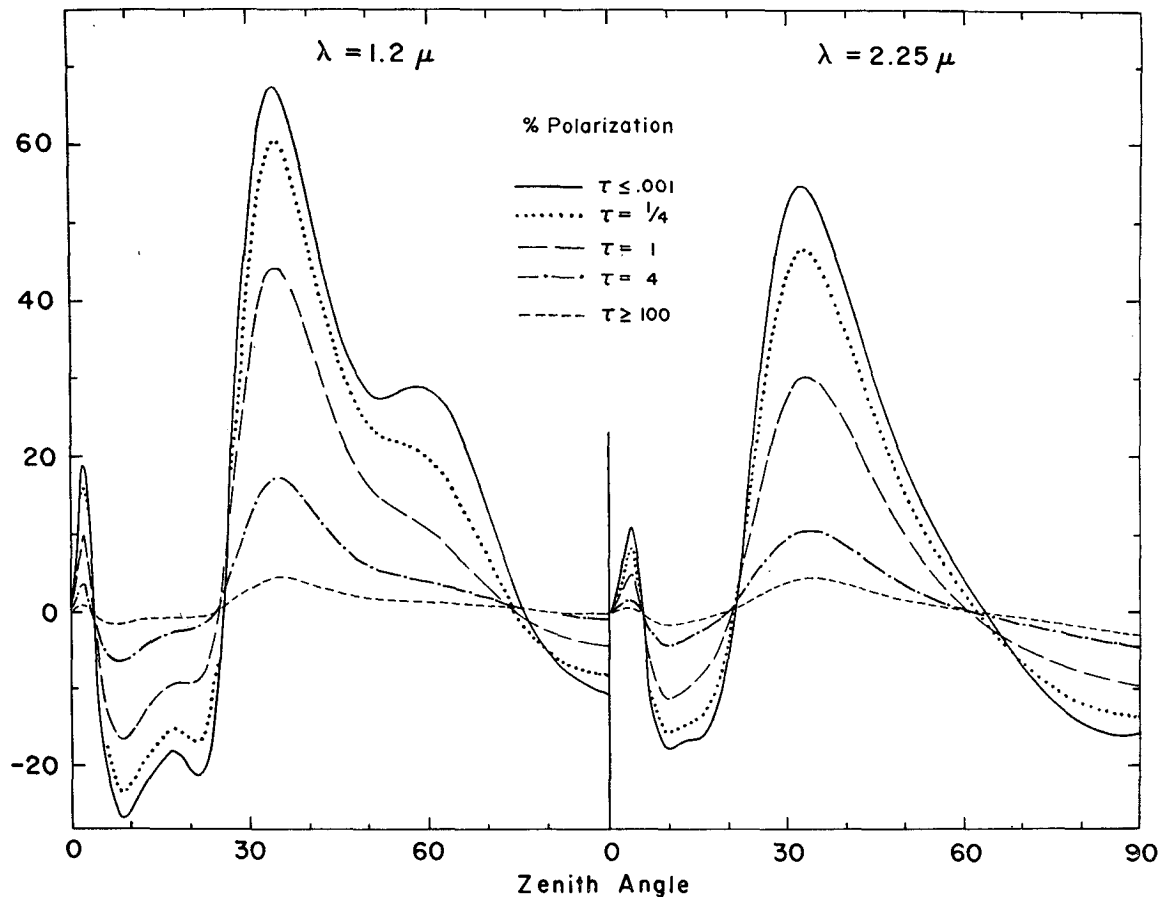


FIG. 8. The polarizations from Figs. 7 and 9 but with a different scale on the vertical axis.

Fig. 7 shows the intensity and polarization at  $\lambda = 1.2 \mu$  for different cloud optical thicknesses. At this wavelength there is a great amount of multiple scattering for thick layers, because the single scattering albedo (Table 2) is near unity. The single scattering features in the angular distribution of the scattered light are therefore practically lost in the intensity graphed on a logarithmic scale. A "limb darkening" for  $\mu \rightarrow 0$  is, however, introduced by the multiple scattering for the reason discussed by Hansen (1969b).

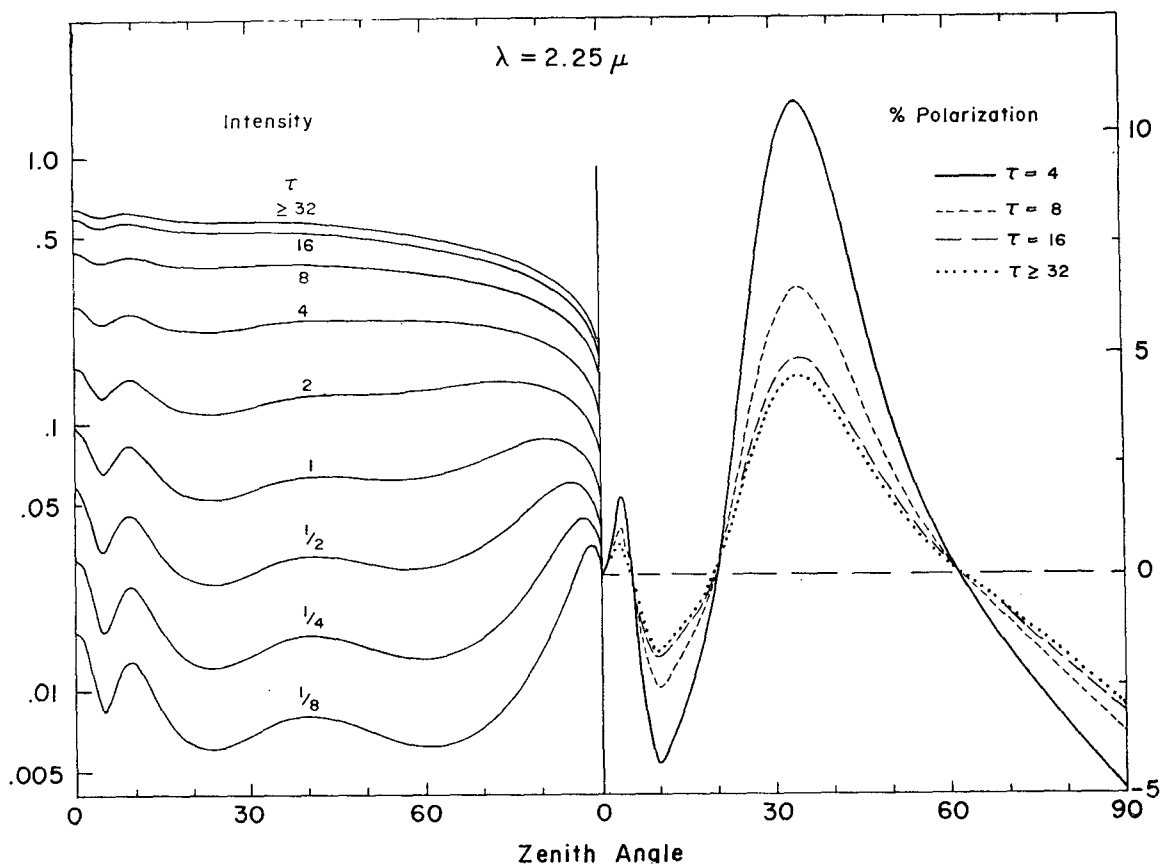
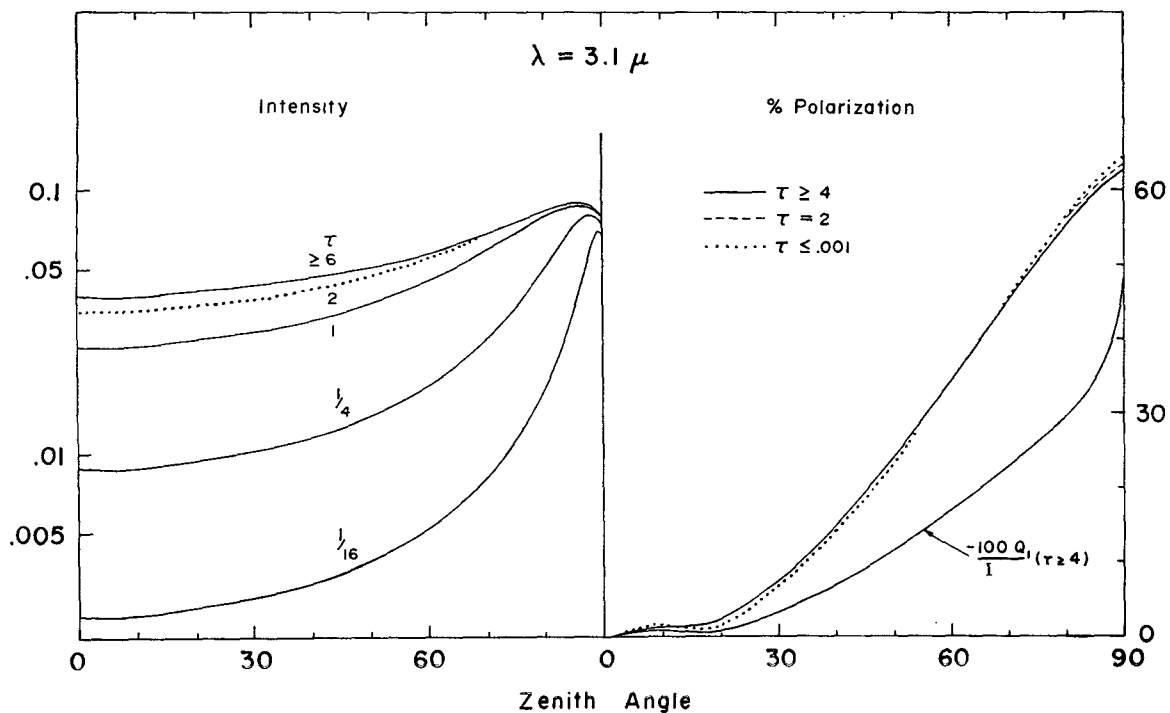
The polarization for  $\lambda = 1.2 \mu$  is plotted in the right half of Fig. 7 for a range of optical thicknesses ( $4 \leq \tau \leq \infty$ ) sufficient to include almost all clouds. It is replotted on the left side of Fig. 8 with a different scale showing all optical thicknesses; Fig. 8 illustrates the change in the single scattering polarization curve and it emphasizes the large reduction in the polarization with increasing optical thickness. It is clear that the primary effect of multiple scattering is to reduce the polarization, as has been anticipated by Lyot (1929), van de Hulst (1949) and Coffeen (1969). Coffeen's assumption, that multiple scattering should not move the zero points of polarization much, holds quite well. However, multiple scattering washes out secondary

features, such as the second rainbow and the supernumerary bow, in the polarization as well as in the intensity.

The format of Fig. 7 and the figures following Fig. 8 are appropriate for comparison to observations, and thus for a practical test of how well single scattering features in the angular distribution of the reflected light survive the smoothing effect of multiple scattering. The intensity is plotted on a logarithmic scale which is consistent both with the presentation of most observers and with the observational accuracies which have been obtained. The polarization is plotted on a linear scale which allows differences of a few tenths of a percent polarization to be resolved, because accuracies of this order are obtained in observations (Lyot, 1929; Coffeen and Gehrels, 1969).

Fig. 9 illustrates the intensity and polarization at  $\lambda = 2.25 \mu$ . The results are quite similar to those at  $\lambda = 1.2 \mu$ . However, at  $2.25 \mu$  the asymptotic ( $\tau \rightarrow \infty$ ) limit is reached at a smaller optical thickness because of the smaller albedo for single scattering (Table 2). The reduction of the polarization due to multiple scattering is also less at  $2.25 \mu$  than at  $1.2 \mu$ .

Fig. 10 shows the intensity and polarization at the

FIG. 9. Same as Fig. 7 except for  $\lambda = 2.25 \mu$ .FIG. 10. Same as Fig. 7 except for  $\lambda = 3.1 \mu$ . In addition, a curve for  $-100 Q_1/I$  is included, where  $Q_1$  refers to first-order (single) scattering and  $I$  is the total intensity including all orders of scattering.

wavelength  $3.1\mu$ , where most of the scattering arises from diffraction and external Fresnel reflection. The polarization is very large because of the high degree of polarization for single scattering and the small amount of multiple scattering. The polarization should thus be easily measurable even considering the problems of the low signal (intensity) and possible thermal emission from the clouds and surroundings. Note that the polarization is essentially independent of the cloud optical thickness. This does not mean that only single scattered photons are present in the reflected light; e.g., Fig. 10 also shows a curve for  $-100Q_1/I = -100Q_1/(I_1+I_2+I_3+\dots)$ , in which all orders of scattering are included in the intensity but only the contribution of single scattering is included in  $Q$ . A comparison of  $-100Q/I$ ,  $-100Q_1/I$  and  $-100Q_1/I_1$  (the curve for  $\tau \leq 0.001$ ) shows that the reflected light for large optical thicknesses contains a significant number of multiple scattered photons, and that these must have a polarization similar to that for single scattering. This suggests that most of the multiple scattered photons in the reflected light suffer their first  $n-1$  scatterings in the diffraction peak (which does not change their direction or polarization much) before their last ( $n$ th) scattering sends them out of the atmosphere. Hansen (1969b), Hansen and Pollack (1970) and Potter (1970) have previously based approximations for multiple scattering on the assumption that diffracted light may be treated as unscattered; in Section 5c we use this assumption in an approximation for the polarization of multiple

scattering which is based on the polarization of single scattering.

At  $\lambda = 3.4\mu$  (Fig. 11), as at  $\lambda = 3.1\mu$ , the results have very little dependence on optical thickness for  $\tau \gtrsim 5$ . Since almost all clouds are at least that thick, this suggests that it may be possible to derive some information about the particles at these wavelengths, e.g., the particle size, and then use the polarization at shorter wavelengths as a measure of the cloud optical thickness.

#### b. Azimuth dependence

For the general case in which the results depend upon the azimuth angle,  $\phi - \phi_0$ , we expand all of the matrices in the doubling method into Fourier series [(26) in Part I]. The series are in practice cut off at some value of  $m$  ( $\equiv M$ ) which depends upon the anisotropy of the single scattering (primarily upon  $\langle r \rangle_{\text{eff}} = a$ ) and upon the angles for which results are desired.

One way to verify that a sufficient number of Fourier terms have been included is to check the single scattering results. The number of Fourier terms required to describe the multiple scattering results within a given percentage error does not exceed the number required to describe single scattering with the same percentage error, because multiple scattered photons generally tend to have a smoother angular distribution than single scattered photons. A second check that a sufficient number of Fourier terms have been included is provided by the fact that the multiple scattering is

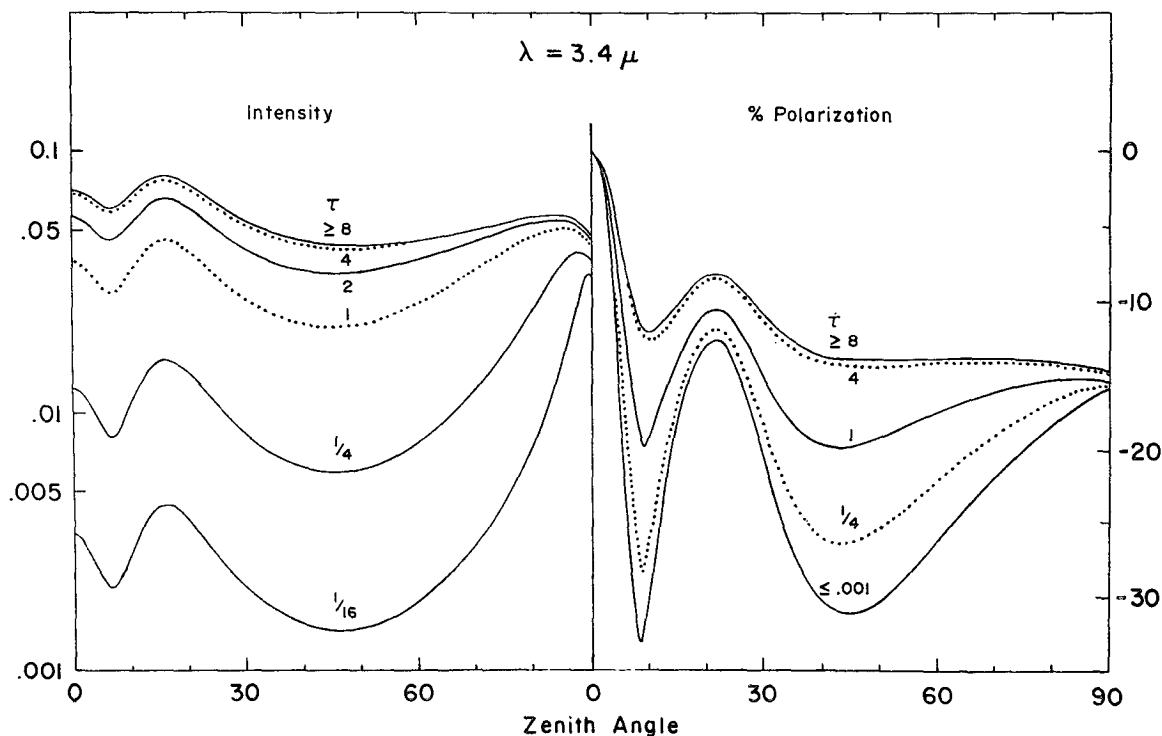


FIG. 11. Same as Fig. 7 except for  $\lambda = 3.4\mu$ .

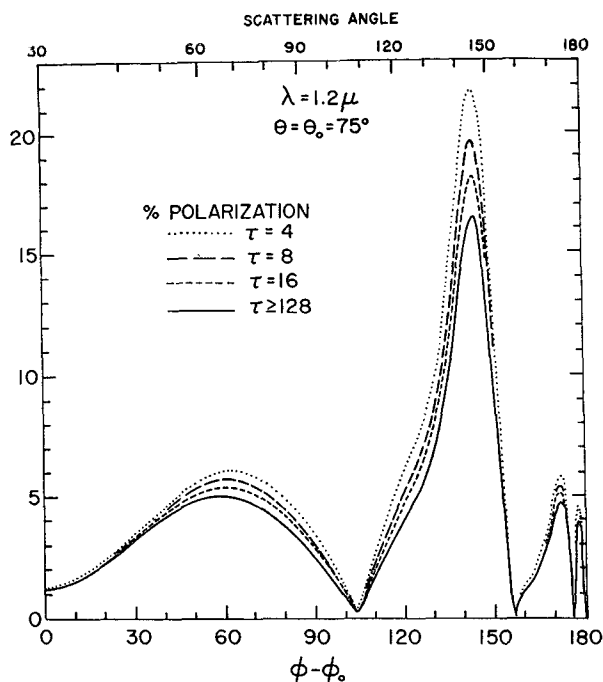


FIG. 12. Percent polarization,  $[100(Q^2 + U^2 + V^2)^{1/2}/I]$ , of sunlight reflected by a plane parallel cloud with  $\theta(\text{arc cos } \mu) = \theta_0(\text{arc cos } \mu_0) = 75^\circ$ . The wavelength is  $1.2 \mu$  and results are shown for several optical thicknesses. The calculations are for the size distribution (1) with  $a = 6 \mu$  and  $b = \frac{1}{3}$ . The scattering angle  $\alpha$  is shown at the top.

computed for the Fourier terms consecutively, i.e., by the fact that the doubling process for a given Fourier term is carried to the total desired optical thickness before the computations are begun for the next Fourier term. Thus, when the point is reached that additional Fourier terms do not significantly change the reflection matrix in any direction, it is an indication that a sufficient number of terms have been included. This is not a mathematician's check, but in practice it works.

The concept of an effective single scattering albedo for each Fourier term has been introduced by van de Hulst (1971) and provides a simple manner of visualizing the computational behavior to be expected from the different Fourier terms. It is clear that photons scattered more and more times will have an increasingly smooth angular distribution and thus will contribute little to the high Fourier terms. Therefore, the effective single scattering albedo tends to decrease toward the higher Fourier terms. This has previously been realized and used as the basis for computational simplifications by Hansen and Pollack (1970) and Dave and Gazdag (1970); indeed, the highest Fourier terms may be accurately described by single scattering alone (Hansen and Pollack, 1970). The same concepts and similar conclusions are valid when polarization is considered, but a more detailed discussion is beyond the scope of this paper.

All of the computations in this section on the azimuth dependence are for the size distribution (1) with  $a = 6 \mu$  and  $b = \frac{1}{3}$ .

Figs. 12 and 13 show the polarization and intensity at  $\lambda = 1.2 \mu$  for a case in which both  $\theta$  and  $\theta_0$  are close to the horizon. For this case the scattering angle, as indicated on the upper part of the figures, goes through the range  $30^\circ \leq \alpha \leq 180^\circ$  while  $0^\circ \leq \phi - \phi_0 \leq 180^\circ$ . Thus, compared to Fig. 7, a greater range of the scattering angle occurs, but this adds only the region of twice-refracted rays to the results. Because of the near grazing directions of  $\theta$  and  $\theta_0$ , single scattering contributes a much larger fraction of the reflected photons than in the case  $\theta_0 = 0^\circ$  (Fig. 7). Therefore, the single scattering features are not as effectively smoothed out by multiple scattering, and the polarization has a higher value.

Fig. 14 shows the polarization at  $\lambda = 1.2 \mu$  for  $\theta = \theta_0 = 30^\circ$ . In this case a range of  $60^\circ$  occurs in the scattering angle. The polarization has a magnitude about the same as when the sun is at the zenith (Fig. 7).

Fig. 15 shows a case in which  $\theta \neq \theta_0$ . The qualitative variation of the polarization is again easily understood on the basis of the phase matrix and the scattering angles involved. This and the other azimuth-dependent plots illustrate that the zero points in the polarization [defined as  $(Q^2 + U^2 + V^2)^{1/2}/I$ ] are usually lost due to the action of multiple scattering. However, the polarization introduced by multiple scattering at these angles is small, and indeed the entire form of single scattering polarization is generally well preserved in the multiple-scattering results.

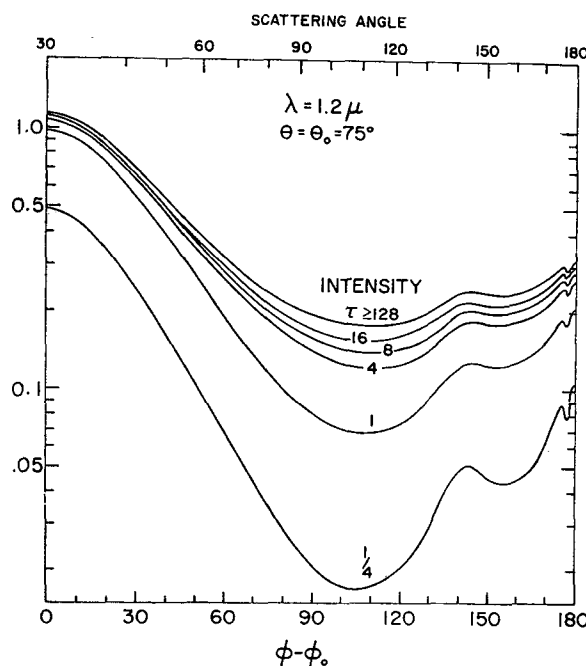
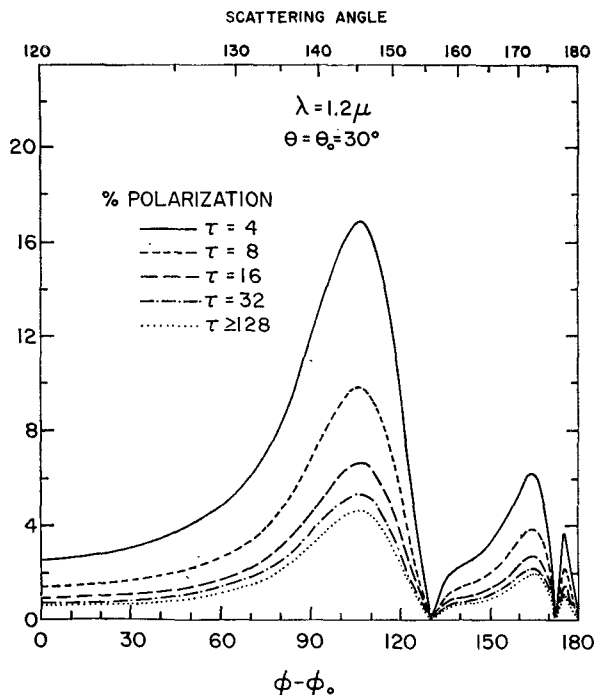
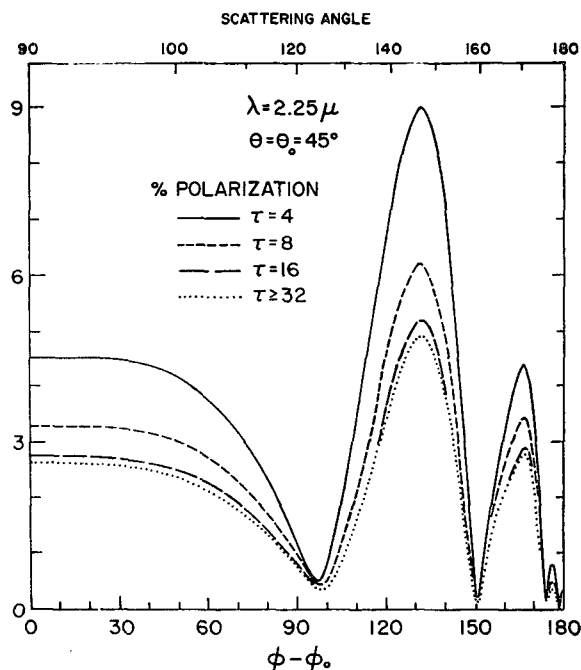


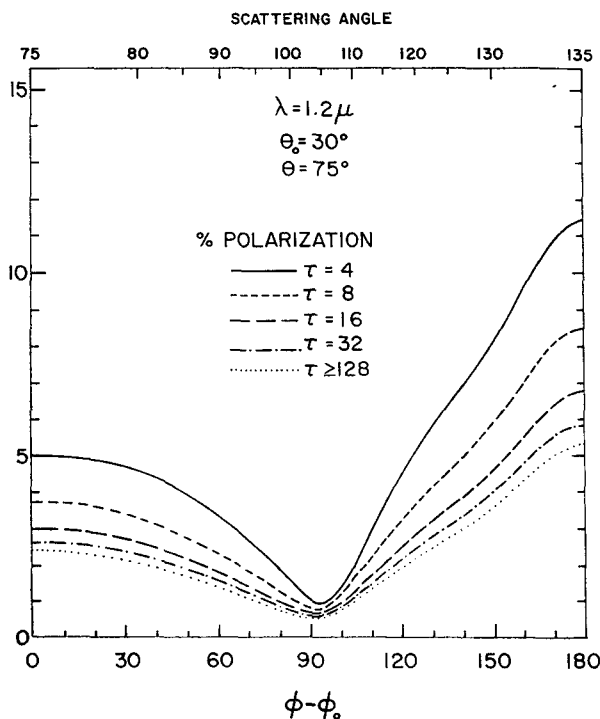
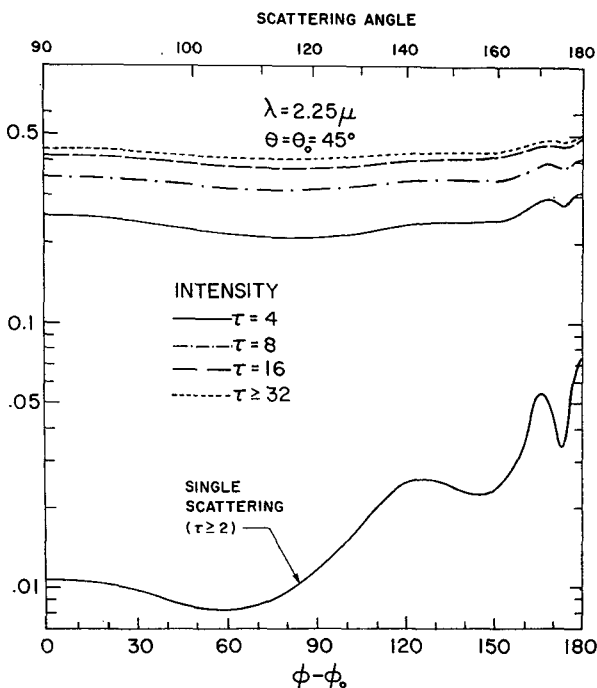
FIG. 13. Same as Fig. 12 except for the intensity,  $I = \mu_0 R^{11}$ .

FIG. 14. Same as Fig. 12 except for  $\theta = \theta_0 = 30^\circ$ .

Figs. 16–18 illustrate azimuth-dependent results for  $\lambda = 2.25 \mu$ . The phase matrix for this case is given in Table 3. Fig. 17 includes the intensity due to single scattering for  $\tau = \infty$ ; this is correct within the thickness of the curve for  $\tau \geq 2$ . This figure shows how the single

FIG. 16. Percent polarization,  $[100(Q^2 + U^2 + V^2)^{1/2}/I]$ , of sunlight reflected by a plane parallel cloud with  $\theta = \theta_0 = 45^\circ$ . The wavelength is  $2.25 \mu$  and results are shown for several optical thicknesses. The calculations are for the size distribution (1) with  $a = 6 \mu$  and  $b = \frac{1}{2}$ . The scattering angle  $\alpha$  is shown at the top.

scattering features are lost in the multiple scattering intensity even for  $\theta = \theta_0 = 45^\circ$ . In cases in which there is considerable multiple scattering,  $\theta$  and  $\theta_0$  must be near the horizon for single scattering features to survive

FIG. 15. Same as Fig. 12 except for  $\theta = 75^\circ$  and  $\theta_0 = 30^\circ$ .FIG. 17. Same as Fig. 16 except for the intensity,  $I = \mu_0 R^{11}$ .

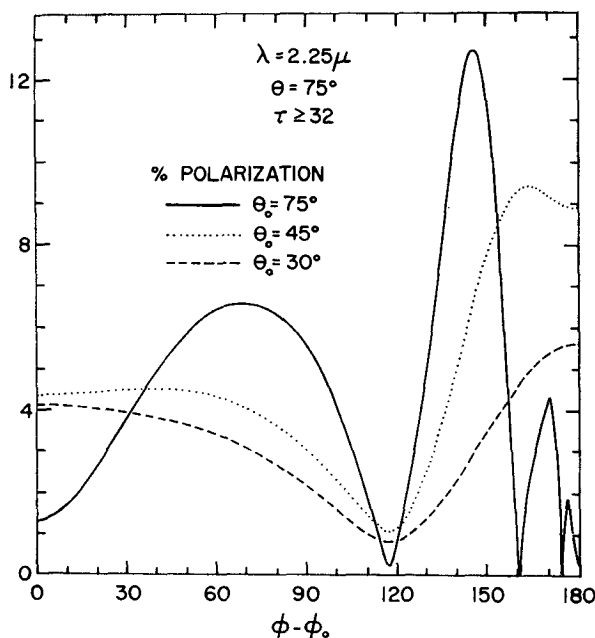


FIG. 18. Percent polarization,  $[100(Q^2 + U^2 + V^2)^{1/2}/I]$ , of sunlight reflected by a plane parallel cloud. The wavelength is  $2.25 \mu$ , the zenith angle of the reflected light is  $75^\circ$  and the optical thickness of the cloud is  $\geq 32$ . Results are shown for three zenith angles of the sun. The calculations are for the size distribution (1) with  $a = 6 \mu$  and  $b = \frac{1}{3}$ .

in the intensity. In the polarization, however, the features due to single scattering are still very strong, as illustrated in Figs. 16 and 18.

Fig. 19 shows the polarization at  $\lambda = 3.4 \mu$  in the principal plane (the plane of scattering, in which  $\phi - \phi_0 = 0^\circ$  or  $180^\circ$ ). The sun is at  $\theta_0 = 45^\circ$ . The polarization is not symmetric about  $\theta = 45^\circ$ , but the deviations from such a symmetry are not very great. This is another example of the close dependence of the polarization on the scattering angle  $\alpha$ , through the phase matrix  $P(\alpha)$ .

The number of Fourier terms included in Figs. 12, 16 and 19 were 120, 60 and 25, respectively. As mentioned above, many of these terms may be obtained with relatively little computation. A detailed discussion of this will be given in a later publication.

### c. Effect of particle size

Figs. 20–22 illustrate the dependence of the intensity and polarization of the reflected light on the particle size. The results are for the optical thickness  $\tau = 32$ , which is within the range typical for water clouds. The effective radius,  $a$  in the distribution (1), is given the values 3, 6, 12 and  $24 \mu$ , while  $b = \frac{1}{3}$  in all cases. The sun is at the zenith,  $\theta_0 = 0^\circ$ .

At  $\lambda = 1.2 \mu$  the reflected intensity decreases with increasing particle size. This is due primarily to a small decrease in the single scattering albedo (Table 2) for the larger particles. The glory and primary rainbow are

stronger for the larger particles, partly because of the reduced multiple scattering and partly because these features are stronger in the single scattering for the larger particles.

The variations of the polarization with effective particle size at  $\lambda = 1.2 \mu$  are more pronounced than the variations of the intensity. In the case  $a = 24 \mu$  the first supernumerary bow is clearly present in the polarization, though the higher bows are reduced to a series of shoulders; the second rainbow is present as a broad shoulder for  $a = 24 \mu$ . For  $a = 6, 12$  and  $24 \mu$ , which comprise the range expected to typify most terrestrial water clouds, there is in each case a strong rainbow and glory.

At  $\lambda = 3.4 \mu$  (Fig. 21) both the intensity and polarization are very sensitive to the particle size. Note that the scale on the polarization differs by a factor of about 4 from that for  $\lambda = 1.2 \mu$ . For the larger particle sizes ( $a = 12$  and  $24 \mu$ ) there are strong positive polarization features due to the rainbow and to external Fresnel reflection; for the smaller particle sizes the polarization is negative at the same scattering angles.

The polarization for  $\lambda = 2.25$  and  $3.1 \mu$  is shown in Fig. 22. At  $\lambda = 2.25 \mu$  the polarization is more strongly dependent on particle size than at  $\lambda = 1.2 \mu$ . At  $\lambda = 3.1 \mu$  the polarization is very large and practically independent of particle size for  $a \gtrsim 12 \mu$ ; for smaller sizes there is a significant dependence of the polarization on  $a$ .

### d. Observed size distributions

We have made some multiple scattering computations for observed cloud particle size distributions.

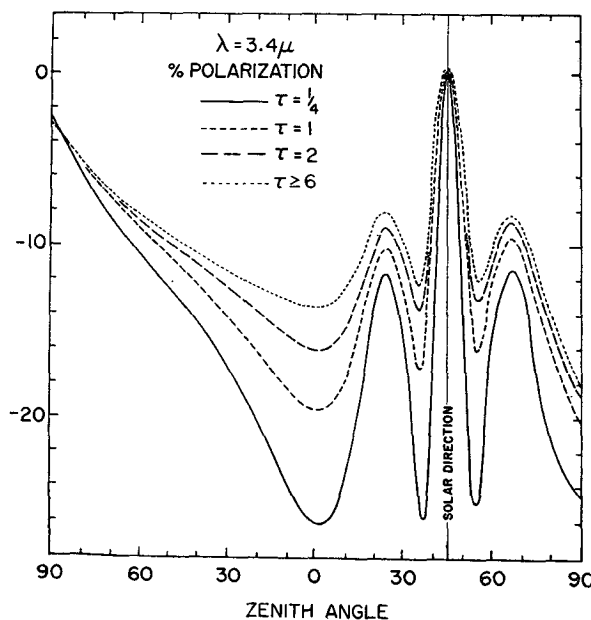


FIG. 19. Percent polarization,  $[100(Q^2 + U^2 + V^2)^{1/2}/I]$ , in the principal plane for sunlight reflected by a plane parallel cloud. The wavelength is  $3.4 \mu$ , and the zenith angle of the sun is  $45^\circ$ .

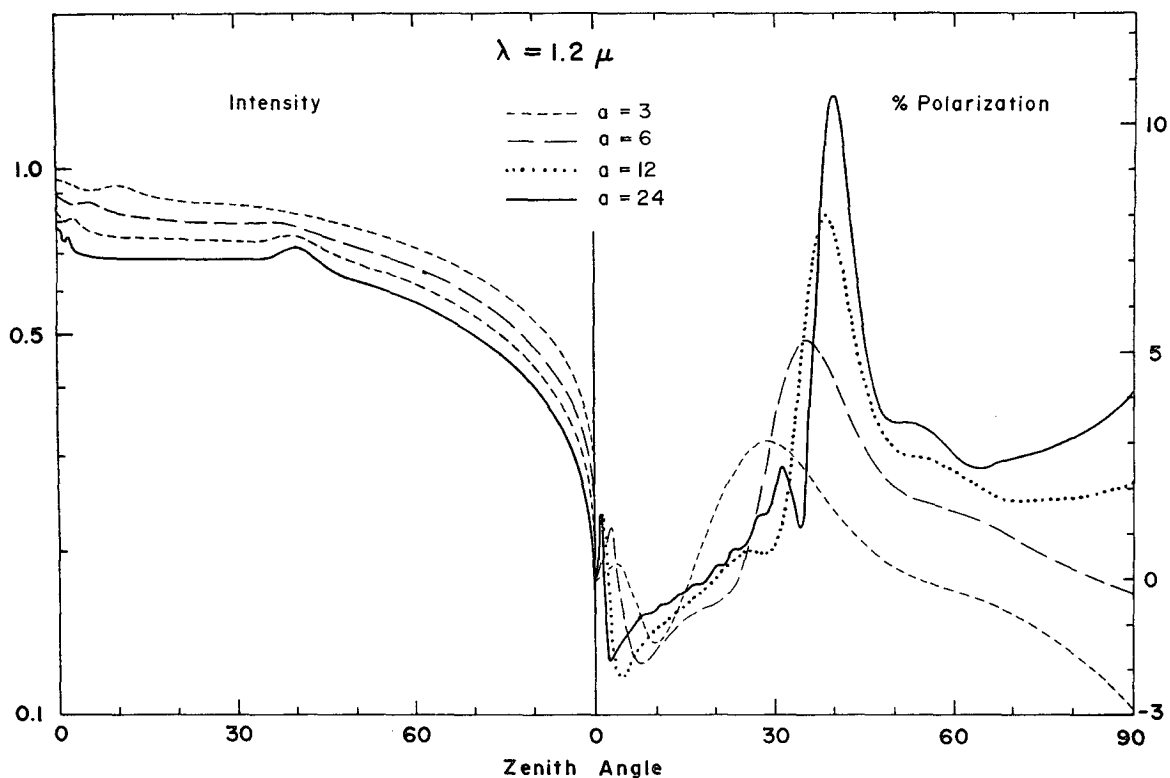


FIG. 20. Intensity ( $I = \mu_0 R^{11}$ ) and percent polarization ( $-100 Q/I = -100 R^{21}/R^{11}$ ) of sunlight reflected by a plane parallel cloud with the sun overhead ( $\theta_0 = 0^\circ$ ). The wavelength is  $1.2 \mu$  and the cloud optical thickness is 32. The calculations are for the size distribution (1) for the four indicated values of  $a$  (in  $\mu$ ), all for  $b = \frac{1}{3}$ . On the horizontal axis is the zenith angle of the reflected light,  $\theta = \cos^{-1} \mu$ .

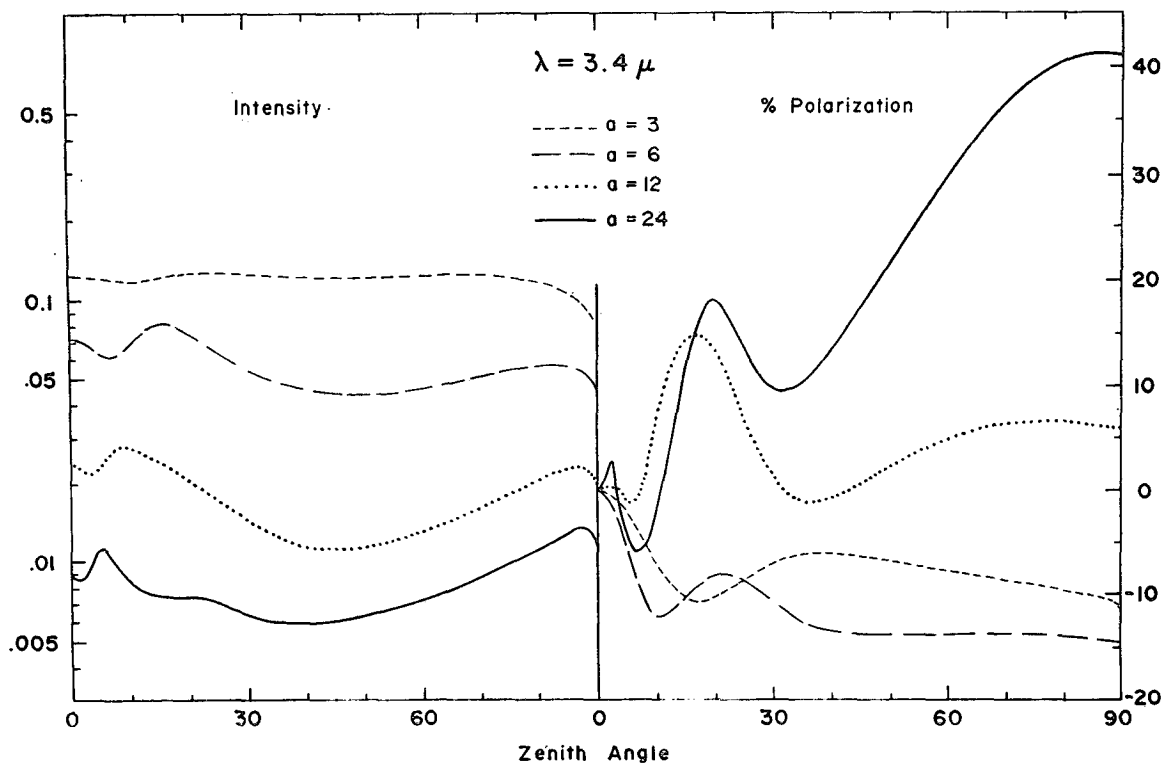


FIG. 21. Same as Fig. 20 except for  $\lambda = 3.4 \mu$ .

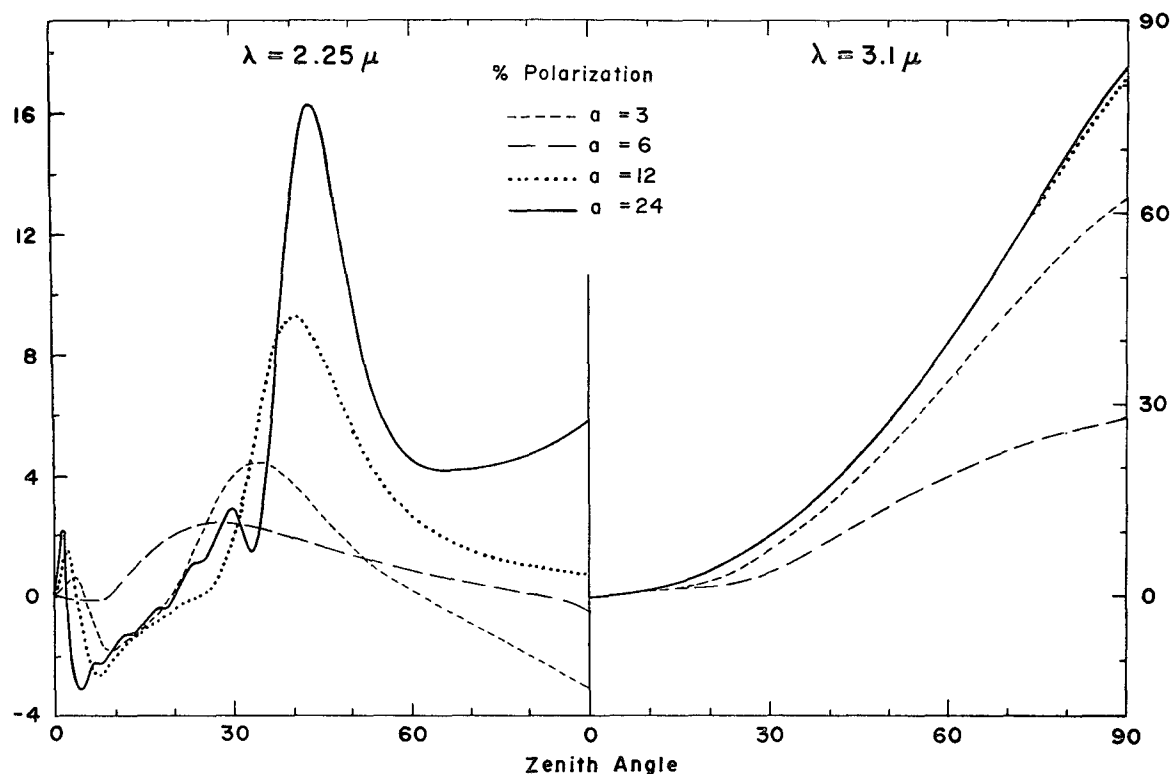


FIG. 22. Percent polarization ( $-100 Q/I = -100 R^{\text{II}}/R^{\text{II}}$ ) of sunlight reflected by a plane parallel cloud with the sun overhead ( $\theta_0 = 0^\circ$ ). Results are shown for two wavelengths, 2.25 and  $3.1\mu$ . The cloud optical thickness is 32. The calculations are for the size distribution (1) for the four indicated values of  $a$  (in  $\mu$ ), all for  $b = \frac{1}{3}$ . On the horizontal axis is the zenith angle of the reflected light,  $\theta = \cos^{-1}\mu$ .

The number of these computations was limited, however, because the generality of the classification into cloud types is uncertain, particularly for particles near the cloud tops.

For Fig. 23 computations were made to illustrate two of the conclusions indicated by the preceding results obtained for the size distribution (1). The size distributions were those reported by Diem (1948) for three cloud types and shown in Fig. 1.

The left side of Fig. 23, for  $\lambda = 3.5\mu$ , illustrates the sensitivity of the polarization to the particle size for this wavelength region. As mentioned in Section 2b some observers report larger particles than those of Diem; therefore, in practice there may be differences in the polarization even larger than those indicated.

The right side of Fig. 23, for  $\lambda = 1\mu$ , illustrates that in this wavelength region there is a strong rainbow in the polarization for all of these cloud particle size distributions. This feature is not expected to be present for ice clouds (Section 3), and hence it should be possible to use it to distinguish between ice and water clouds.

## 5. Approximations for multiple scattering

### a. Intensity with polarization neglected

Much of the theoretical work in light scattering has been for the case in which the intensity is treated as a

quantity for which the multiple scattering can be computed independently of the other Stokes parameters. This case is a hypothetical one which does not occur in nature, because when light is scattered it, in general, becomes polarized. However, the neglect of polarization enormously simplifies the theoretical work; hence, this scalar approximation can be a very valuable one when it is only required to obtain the intensity. It is therefore essential to determine the accuracy of the intensity computed in this approximation.

Chandrasekhar (1960) computed the intensity for Rayleigh scattering using both an exact theory with polarization and the scalar approximation. He found that it was not unusual for the differences in these intensities to be  $\sim 5\%$ . Errors of this order are not always negligible. However, scattering by particles as large or larger than the wavelength presents an entirely different case for which the scalar approximation must be reexamined.

Kattawar and Plass (1968) used the Monte Carlo method to compute the intensity of light reflected by cloud and haze particles, both with polarization and in the scalar approximation. Their results (Figs. 7 and 11 in their paper) show some differences of  $\sim 10\%$  for the intensities in these two cases; for grazing directions the differences are often  $> 10\%$ , but at most other

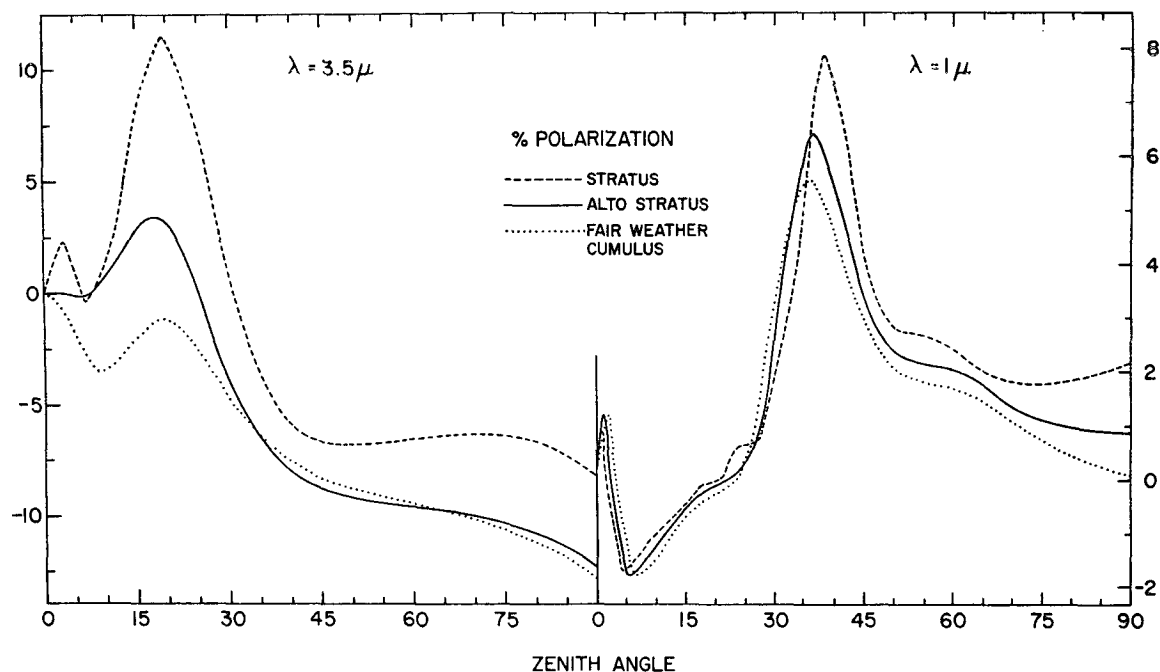


FIG. 23. Percent polarization ( $-100 Q/I = -100 R^{\text{H}}/R^{\text{V}}$ ) of sunlight reflected by a plane parallel cloud with the sun overhead ( $\theta_0 = 0^\circ$ ). Results are shown for two wavelengths, 3.5 and  $1 \mu$ . The cloud optical thickness is 32. The calculations are for three size distributions reported by Diem (1948) and shown in Fig. 1. On the horizontal axis is the zenith angle of the reflected light,  $\theta = \cos^{-1} \mu$ .

angles the differences are  $< 10\%$ . Kattawar and Plasse point out that many of these differences must be due to statistical fluctuations in the Monte Carlo results, and they conclude that the errors in the scalar approximation should be small provided that the average single scattering polarization is not too large.

We have also compared the intensities obtained in the case in which polarization is correctly accounted for and in the scalar approximation in which polarization is neglected. Both of these cases were included in all of our multiple scattering computations for this paper. Thus, wide ranges in the size parameter and optical properties were included, and the results can be used for some fairly general conclusions.

We found the difference in these two intensities to be generally  $\lesssim 1\%$ . The magnitude of this difference, however, depended on the wavelength (optical properties), optical thickness and particle size; in most cases the differences were much less than  $1\%$ . We used two methods to compare these intensities. First both intensities were plotted automatically on the same diagram, and no cases were found in which the two curves could be distinguished. The resolution of this method was, however, limited to  $\sim 1\text{--}2\%$ . In order to obtain a more precise comparison we also examined the computed numbers at several different angles. On the basis of checks including variations of the computational parameters we believe that the accuracy was always sufficient to distinguish differences of  $0.01\%$  in the two intensities.

The error in the scalar approximation was found to have a predictable dependence on optical thickness. For  $\tau \rightarrow 0$  the error disappeared because the single scattering intensity is identical in the exact method and the scalar approximation. The largest percent error occurred for  $\tau \approx 1$ . The percent error tended to decrease for larger optical thicknesses, particularly at  $\lambda = 1.2$  and  $2.25 \mu$ . This decrease is understandable since photons scattered many times are essentially unpolarized and contribute almost equally to the exact intensity and the scalar intensity.

At  $\lambda = 1.2$  and  $2.25 \mu$  the error in the scalar approximation was typically  $\sim 0.1\%$ . For  $\tau \approx 1$  the error was a few tenths of a percent for some angles. None of the angles and optical thicknesses which we checked showed an error as large as  $1\%$ . The magnitude of the error had little dependence on the particle size. It is clear that the errors in the scalar approximation would be of this same order for scattering by clouds at shorter wavelengths.

The largest errors which we found in the scalar approximation were for  $\lambda = 3.1 \mu$ , where the polarization for single scattering is very high. In this case errors of  $\sim 1\%$  were common, and in some cases we found errors of  $\sim 2\%$ . At this wavelength the errors tended to decrease with increasing particle size, a consequence of the increasing anisotropy of single scattering (see Table 2 and the discussion below). At  $\lambda = 3.4 \mu$  the errors were intermediate between those at  $\lambda = 3.1 \mu$  and those

at  $\lambda = 1.2$  and  $2.25 \mu$ ; however, in most cases the errors at  $\lambda = 3.4 \mu$  did not exceed 1%.

Thus, the intensity of reflected light in the scalar approximation is much more accurate for scattering by clouds, than in the case of Rayleigh scattering. This difference can be accounted for by the influence of two factors: the greater amount of forward scattering by the cloud particles, and their lesser polarization of single scattering. It is photons scattered a small number of times, but more than once, which have the greatest differences between the scalar intensity and the exact intensity. For an optically thick layer of high albedo the photons scattered a small number of times represent a fraction of the total number of reflected photons which decreases with increasing forward scattering; for conservative scattering (Hansen, 1970) this fraction varies approximately as  $(1 - \langle \cos \alpha \rangle)$ .

It seems clear that the error in the scalar approximation should be comparable for nonspherical and spherical particles. The same differences compared to Rayleigh scattering, the greater forward scattering and the lesser polarization of single scattering exist for nonspherical particles. Thus, in most cases the error in the scalar approximation should be  $\lesssim 1\%$  for reflection from a cloud of particles which are at least as large as the wavelength.

#### b. Intensity and polarization with $P^{43}(\alpha) = 0 = P^{34}(\alpha)$

For Rayleigh scattering the phase matrix elements  $P^{43}(\alpha)$  and  $P^{34}(\alpha)$  are identically zero; hence, in  $\mathbf{P}(\mu, \mu_0, \phi - \phi_0)$  [i.e., in the phase matrix referred to the meridian plane and given by (23) in Part I] the only nonzero matrix element in the fourth row or fourth column is  $P^{44}(\mu, \mu_0, \phi - \phi_0)$ . Thus, the same is true for  $\mathbf{R}(\mu, \mu_0, \phi - \phi_0)$  and  $\mathbf{T}(\mu, \mu_0, \phi - \phi_0)$ , and Rayleigh scattering is reducible to a problem with three-by-three matrices plus a problem with one-by-one matrices (i.e., scalars).<sup>4</sup> This allows a reduction in the work involved in obtaining a solution for multiple scattering, and in many cases, e.g., when the incident light is unpolarized, there is little reason for solving the scalar part of the problem.

For Mie scattering a corresponding reduction is not strictly possible because  $P^{43}(\alpha) = -P^{34}(\alpha) \neq 0$ . However, for scattering by spherical particles  $P^{43}(\alpha)$  and  $P^{34}(\alpha)$  usually have a smaller numerical value than the diagonal matrix elements,  $P^{11}(\alpha)$  and  $P^{33}(\alpha)$ , at most scattering angles. Furthermore, for unpolarized incident light  $P^{43}(\alpha)$  and  $P^{34}(\alpha)$  do not contribute in the first-order (single) scattering to the Stokes parameters of the reflected light;  $P^{43}(\alpha)$  and  $P^{34}(\alpha)$  contribute only through the "mixing" of matrix elements which occurs with multiple scattering. This contribution may be quite small because of the relatively small value of

$P^{43}(\alpha)$  and  $P^{34}(\alpha)$ . Therefore, it is worthwhile to investigate the approximation  $P^{43}(\alpha) = 0 = P^{34}(\alpha)$ . We call this the three-by-three approximation.

We have made computations in the three-by-three approximation for comparison to computations in the exact (four-by-four) problem. For both problems the computations were made at  $\lambda = 1.2, 2.25, 3.1$  and  $3.4 \mu$ , and at each of these wavelengths for  $a = 3, 6, 12$  and  $24 \mu$  in the size distribution (1), with  $b = \frac{1}{9}$  in all cases. Thus, wide ranges of the size parameter and optical properties were considered. The Stokes parameters and the degree of polarization were printed out for the nine sets of zenith angles resulting from  $\theta$  and  $\theta_0$  equal<sup>5</sup> to  $30^\circ, 45^\circ$  and  $75^\circ$ ; in each case results were printed for  $\tau = \frac{1}{4}, 1$  and  $32$ , at  $\sim 20$  values of  $\phi - \phi_0$  in the range  $0^\circ \leq \phi - \phi_0 \leq 180^\circ$ . The results were compared for at least several values of  $(\theta, \theta_0, \phi - \phi_0)$  for all combinations of  $(\lambda, a, \tau)$ .

We believe that our accuracy was sufficient to detect errors of  $10^{-8}$  or greater in the intensity in the three-by-three approximation; the error is defined here as

$$|I(\text{three-by-three}) - I(\text{four-by-four})| / I(\text{four-by-four}).$$

This accuracy was indicated by the results of varying the computational parameters. We found that the errors in the three-by-three approximation were typically  $10^{-7}$ – $10^{-8}$ . The error did not reach  $10^{-6}$  for any of the wavelengths, particle sizes and optical thicknesses which we considered. In the limit of small particles the three-by-three approximation is exact, and the size parameters which we considered included cases approaching the limit of geometrical optics. We therefore conclude that the intensity in the three-by-three approximation is accurate to at least one part in  $10^6$  for Mie scattering phase matrices and incident unpolarized light, at least for the range of optical properties considered.

We believe that the accuracy was sufficient to detect errors  $\geq \pm 0.000001$  in the degree of polarization,  $(Q^2 + U^2 + V^2)^{1/2} / I$ . At  $\lambda = 1.2$  and  $2.25 \mu$  we found that the errors were  $\lesssim 0.0002$  in the degree of polarization for the three-by-three approximation. At  $\lambda = 3.1 \mu$  the errors were  $\lesssim 0.00001$ , while at  $\lambda = 3.4 \mu$  they were  $\lesssim 0.00002$ . Since the three-by-three approximation yields  $V = 0$ , it may be assumed that it gives more accurate results as an approximation for the degree of linear polarization,  $(Q^2 + U^2)^{1/2} / I$ , than as an approximation for the total polarization. This was found to be the case, but the improvement was not very great and the error limits given above describe the accuracy for the linear polarization as well as for the total polarization.

The errors in the intensity and degree of linear polarization in the three-by-three approximation are

<sup>4</sup> Further reductions are also possible in the special case of Rayleigh scattering (Chandrasekhar, 1960; Sekera, 1966) but they are not required for the present discussion.

<sup>5</sup> In the azimuth-independent case,  $\theta = 0^\circ$  or  $\theta_0 = 0^\circ$ , the three-by-three approximation is exact for a Mie scattering phase matrix and incident unpolarized light.

obviously negligible for most practical applications. Thus, for comparison to observations of the polarization of sunlight reflected by water clouds, it is adequate to make theoretical computations with three-by-three matrices. This simplification is important; e.g., in the doubling method it reduces the computation time by a factor somewhat greater than 2 and it reduces the required computer storage (memory) space by a factor somewhat less than 2. Of course, if the Stokes parameter  $V$  is needed, the computations must be made with the full four-by-four matrices.

### c. First-order scattering

It is known that most of the polarization of light reflected by an optically thick cloud is due to photons scattered once or a small number of times. Photons scattered many times tend to be moving in random directions and to be unpolarized. Lyot (1929) verified experimentally that if the optical thickness is increased the primary effect on the polarization is a simple reduction in the degree of polarization. van de Hulst (1957, p. 442) emphasized that the reduction factor should depend on the directions of the incident and emergent light. To avoid the problem of determining this reduction factor, Coffeen (1969) suggested that the zero points of the polarization be studied, because these do not move in angular location if multiple scattered photons are unpolarized.

A test of the assumption that multiple scattered photons are unpolarized may be obtained by comparing

$$\frac{(Q_1^2 + U_1^2 + V_1^2)^{\frac{1}{2}}}{I}$$

to the degree of polarization computed in the previous parts of this paper. We call the above quantity the "first-order" approximation for the polarization, although  $I$  includes all orders of scattering. This first-order approximation was computed alongside all of the multiple scattering computations reported in this paper. The comparisons show that the first-order approximation yields a polarization with the same general appearance as that of the correct polarization and that Coffeen's assumption is quite accurate for scattering by clouds, i.e., multiple scattering does not move the zero points of the polarization much. However, the values of the polarization in the first-order approximation are commonly in error by a factor of 2 or more. Furthermore, we illustrated in Fig. 10 a case in which the multiple scattered photons have a polarization almost identical to that of single scattered photons! This is an extreme opposite of the assumption that multiple scattered photons are unpolarized.

Fig. 10 suggests that an improved version of the first-order approximation could be obtained for scattering by cloud particles if photons scattered in the forward diffraction peak were counted as being unscattered

(Section 4a) in computing  $Q$ ,  $U$ , and  $V$ ; then the possibility that such photons contribute to  $Q$ ,  $U$  and  $V$  in their next scattering can be easily accounted for. The fraction of photons in the forward peak for single scattering is defined as

$$f = \int_{4\pi} (P^{11} - P_{\text{trn}}^{11}) \frac{d\omega}{4\pi} \quad (9)$$

where  $P_{\text{trn}}^{11}$  is the truncated phase function obtained by extrapolating  $P^{11}$  linearly in Figs. 3–6 from  $\alpha = 25^\circ$  to  $\alpha = 0^\circ$ . For the modified first-order approximation we take

$$\begin{aligned} Q_{1,\text{mod}} &= \frac{\mu_0 \tilde{\omega}_0}{4(\mu + \mu_0)} \left\{ 1 - \exp \left[ -\tau_{\text{mod}} \left( \frac{1}{\mu} + \frac{1}{\mu_0} \right) \right] \right\} \\ &\quad \times P^{21}(\mu, \mu_0, \phi - \phi_0) [1 + \tilde{\omega}_0 f + (\omega_0 f)^2 + \dots] \\ &= \frac{\mu_0 \tilde{\omega}_0}{4(\mu + \mu_0)} \left\{ 1 - \exp \left[ -\tau_{\text{mod}} \left( \frac{1}{\mu} + \frac{1}{\mu_0} \right) \right] \right\} \\ &\quad \times P^{21}(\mu, \mu_0, \phi - \phi_0) / (1 - \tilde{\omega}_0 f), \quad (10) \end{aligned}$$

where

$$\tau_{\text{mod}} = \tau(1 - \tilde{\omega}_0 f). \quad (11)$$

Expressions similar to (10) hold for  $U_{1,\text{mod}}$  and  $V_{1,\text{mod}}$ , but with  $P^{21}$  replaced by  $P^{31}$  and  $P^{41}$ , respectively. (For Mie scattering particles  $P^{41}$  and hence  $V_1$  and  $V_{1,\text{mod}}$  are identically zero.) The polarization in the modified first-order approximation is then

$$\frac{(Q_{1,\text{mod}}^2 + U_{1,\text{mod}}^2 + V_{1,\text{mod}}^2)^{\frac{1}{2}}}{I}$$

The intensity  $I$ , of course, may be obtained in the scalar approximation (Section 5a) with no significant loss of accuracy. Also note that the modified first-order approximation is only intended for application to cases in which the particle size parameter is large enough for a diffraction peak to exist.

We compared the modified first-order approximation to all of the multiple scattering computations in which the phase matrix had a diffraction peak. Typical results are shown in Figs. 24 and 25 which also include the first-order approximation. At  $\lambda = 3.1 \mu$  the modified first-order approximation is a significant improvement over the first-order approximation, as anticipated. At the other wavelengths the modified approximation represents an improvement at most scattering angles. However, it tends to overestimate the polarization in a sharp feature like the glory, because the diffraction peak is at least as broad as the glory. For scattering angles in the region of twice refracted rays ( $20^\circ \lesssim \alpha \lesssim 90^\circ$ ) the modified approximation still underestimates the polarization, apparently because much of the polarization in that region comes from photons scattered a

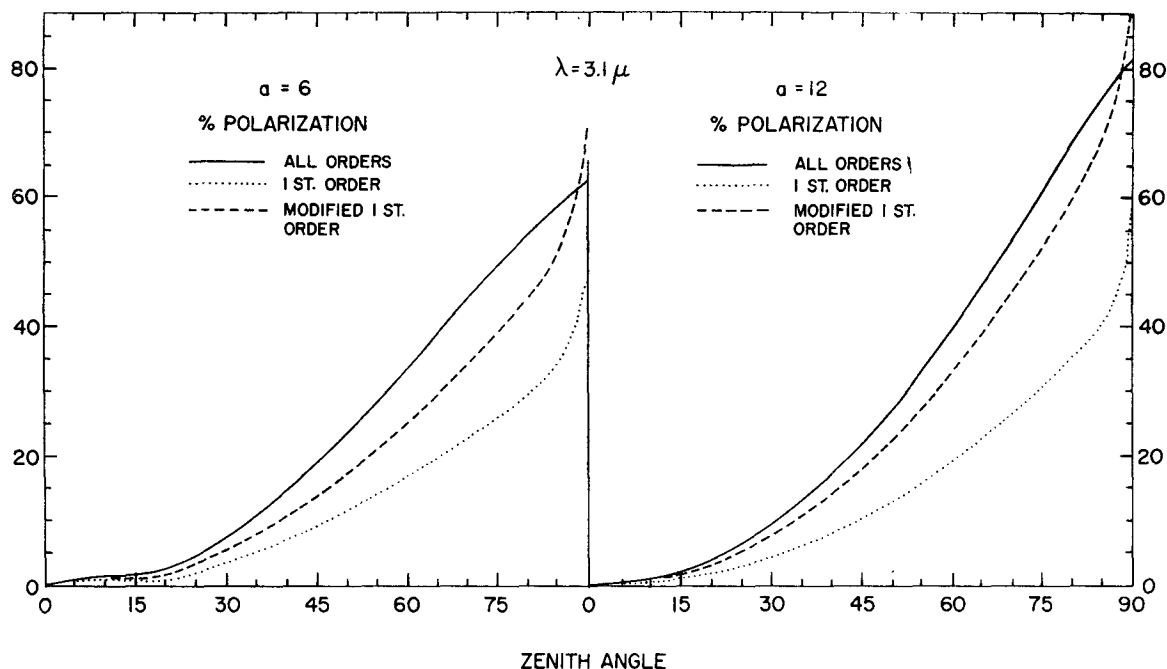


FIG. 24. Percent polarization of sunlight reflected by a plane parallel cloud with sun overhead ( $\theta_0 = 0^\circ$ ). The wavelength is  $3.1 \mu$  and the cloud optical thickness is 32. The calculations are for the size distribution (1) for the two indicated values of  $a$  (in  $\mu$ ), in both cases for  $b = \frac{1}{3}$ . On the horizontal axis is the zenith angle of the reflected light,  $\theta = \cos^{-1}\mu$ . The curves for all orders are  $-100 Q/I = -100 R^{21}/R^{11}$ , the curves for first order are  $-100 Q_1/I = -100 R_1^{21}/I$ , and the curves for the modified first order are  $-100 Q_{1,\text{mod}}/I$ , where  $Q_{1,\text{mod}}$  is defined by (10).

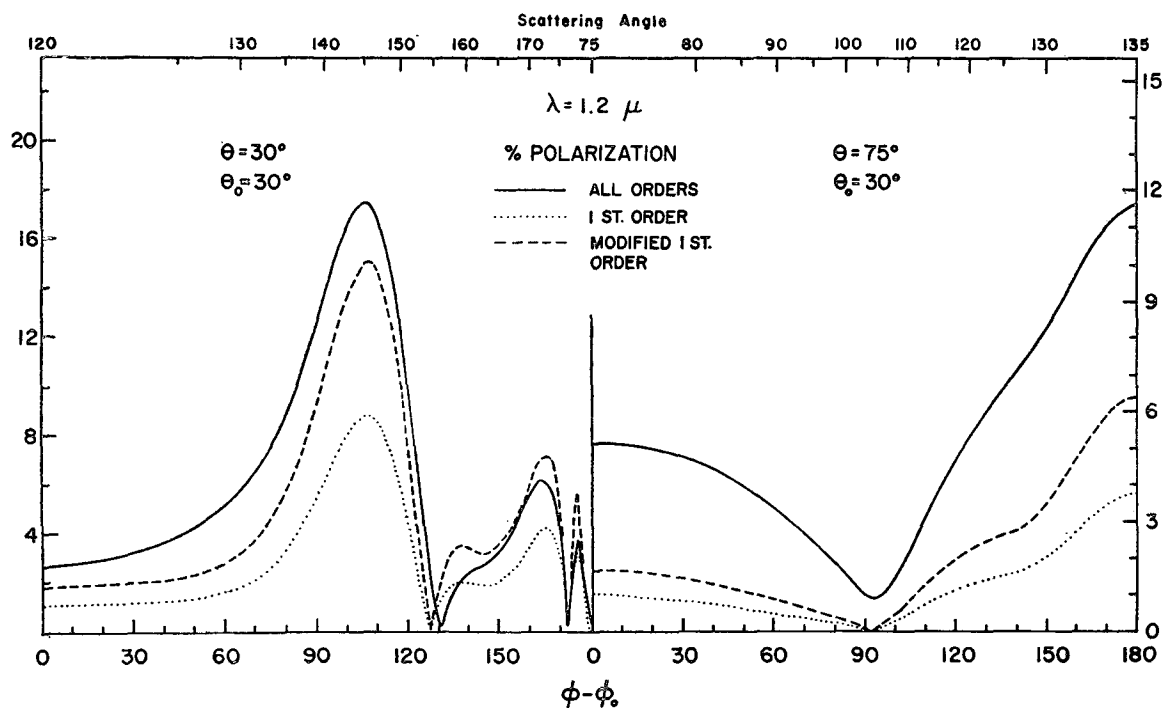


FIG. 25. Percent polarization of sunlight reflected by a plane parallel cloud for the indicated values of  $\theta = \cos^{-1}\mu$  and  $\theta_0 = \cos^{-1}\mu_0$ . The wavelength is  $1.2 \mu$  and the optical thickness is  $\tau = 4$ . The calculations are for the size distribution (1) with  $a = 6 \mu$  and  $b = \frac{1}{3}$ . The three curves have the same meaning as in Fig. 24 except that here the percent polarization is  $100(Q^2 + U^2 + V^2)/I$ .

small number of times with more than one of the individual scatterings in the range from 20–90°.

For cases in which it is not practical to obtain the exact multiple scattering polarization the modified first-order approximation is possibly of some value, because it is no more difficult to apply than the first-order approximation. The modified approximation was also of some use here in indicating which photons cause the polarization in the exact solution. In most cases, however, there is little incentive for applying the approximation since exact solutions are attainable.

#### d. Renormalization approximation

The doubling method is an exact method in the sense that accuracies of several decimals can be obtained if a sufficient number of points are used in the integrations over  $\theta$  and  $\phi$  (Part I). For example, in the case of Rayleigh scattering, for which accurate numbers are available for comparison (Chandrasekhar, 1960; Abhyankar and Fymat, 1970), there is no difficulty in matching the full accuracy (4–5 decimals) of the comparison numbers even in the case of parameter values which are the most difficult for the doubling method ( $\tilde{\omega}_0 = 1$ ,  $\tau = \infty$ ).

For strongly anisotropic phase matrices, however, the number of points required in the integrations over  $\theta$  and  $\phi$  become quite large, in some cases  $\gtrsim 10^2$ . The use of this many points requires both optimal programming and a powerful computer. Since this combination is not easily attainable for all potential users, it is important to find methods of reducing the number of points in the integrations while maintaining an accuracy in the results which is adequate for practical applications. The greatest need is to limit the number of points used for  $\theta$ , because the computation time is very sensitive to this number. Twomey *et al.* (1966) and Hunt (1971) have emphasized this need and they employ computational methods which allow a small number of such points to be used for a sacrifice in the accuracy of the results.

We describe here a computational method which we have previously found useful in the case in which polarization is neglected, and we make some tests of its accuracy with polarization included. The method consists only of replacing the phase function (or the phase matrix when polarization is included) with a modified form; otherwise, no changes are made in the computational method described in Part I.

For convenience we add the subscript  $r$  or  $t$  to the phase matrix to indicate whether it refers to reflection or transmission. Thus,  $\mathbf{P}_r$  is the phase matrix for reflection for which the scattering angle  $\alpha_r$  is given by

$$\cos \alpha_r = -\mu\mu_0 + (1-\mu^2)^{1/2}(1-\mu_0^2)^{1/2} \cos(\phi - \phi_0),$$

and  $\mathbf{P}_t$  is the phase matrix for transmission for which the scattering angle  $\alpha_t$  is given by

$$\cos \alpha_t = \mu\mu_0 + (1-\mu^2)^{1/2}(1-\mu_0^2)^{1/2} \cos(\phi - \phi_0).$$

For a phase matrix known in tabular form,  $\mathbf{P}_r(\alpha_r)$  and  $\mathbf{P}_t(\alpha_t)$  may be obtained by interpolation. The matrices  $\mathbf{P}_r(\mu, \mu_0, \phi - \phi_0)$  and  $\mathbf{P}_t(\mu, \mu_0, \phi - \phi_0)$ , referred to the meridian plane, are obtained from  $\mathbf{P}_r(\alpha_r)$  and  $\mathbf{P}_t(\alpha_t)$  using (23) in Part I. For the method described in Part I  $\mathbf{P}_r(\mu, \mu_0, \phi - \phi_0)$  and  $\mathbf{P}_t(\mu, \mu_0, \phi - \phi_0)$  are needed only at the discrete values of  $\mu$  and  $\mu_0$  corresponding to the Gauss points on the interval (0,1). These discrete points are designated here by  $\mu_i$  and  $\mu_j$ , with  $i$  and  $j$  ranging from 1 to  $L$ , where  $L$  is thus the number of Gauss points used for the zenith angles.

If  $L$  is too small the results in the doubling method are inaccurate, particularly for thick layers and conservative, or nearly conservative, scattering. We have found, however, that one way to significantly improve the accuracy of the results is to multiply  $\mathbf{P}_t(\mu_i, \mu_j, \phi - \phi_0)$  [or, equivalently, each Fourier component  $\mathbf{P}_t^m(\mu_i, \mu_j)$ ] by a factor  $f_{ij}$  such that for each incident direction  $\mu_j$  the probability of single scattering into one of the discrete directions  $\mu_i$  is  $\tilde{\omega}_0$ . The factor  $f_{ij}$  is obtained numerically as described in Appendix B. We note that: 1)  $f_{ij} = f_{ji}$ , hence  $\mathbf{R}$  and  $\mathbf{T}$  retain their proper symmetries; 2) in the limit  $L \rightarrow \infty$ , we have  $f_{ij} \rightarrow 1$ ; and 3)  $\mathbf{P}_r$  is not modified, hence the reflection arising from single scattering is exact. This procedure of replacing  $\mathbf{P}_t^m(\mu_i, \mu_j)$  by  $f_{ij}\mathbf{P}_t^m(\mu_i, \mu_j)$  is essentially a renormalization of the phase matrix which allows the albedo of a layer to be accurately rendered for small values of  $L$  even after many doublings. If this renormalization were not made, then when  $L$  is small the doubling method could yield results which diverge far from the correct solution as  $\tau$  increases. The price paid for keeping the albedo accurate is a somewhat distorted angular distribution of the scattered light. We could loosely term this computational method a discrete ordinate approximation because the method allows stable computations to be made even for a small number of discrete zenith directions, but it is more accurate to call it a renormalization method. This method for renormalizing the phase matrix is apparently closer to that of Twomey *et al.* (1966) than to that of Hunt (1971).

Fig. 26 illustrates the effect of varying  $L$  at  $\lambda = 2.25 \mu$  for the size distribution (1) with  $a = 6 \mu$  and  $b = \frac{1}{9}$ . The results<sup>6</sup> are essentially exact for graphical purposes for  $L \geq 14$ . If the doubling method is used without employing the renormalization factor  $f_{ij}$  it is necessary to take  $L = 30$  to obtain a similar accuracy. Differences of at least a factor of 2 in the values required for  $L$  in these two cases (i.e., with the factor  $f_{ij}$  and without it) are common for thick clouds with a high single scattering albedo; for a thinner cloud or a smaller  $\tilde{\omega}_0$  the differences are less dramatic. However, we did not find any cases in which a larger value of  $L$  is required in the renormalization approximation (i.e., with the factor  $f_{ij}$ ) than in the unmodified doubling method to obtain a

<sup>6</sup> The phase matrix for this case is given in Table 3. In the renormalization approximation it is sufficient to use a linear interpolation to obtain  $\mathbf{P}(\alpha)$  from the tabulated values.

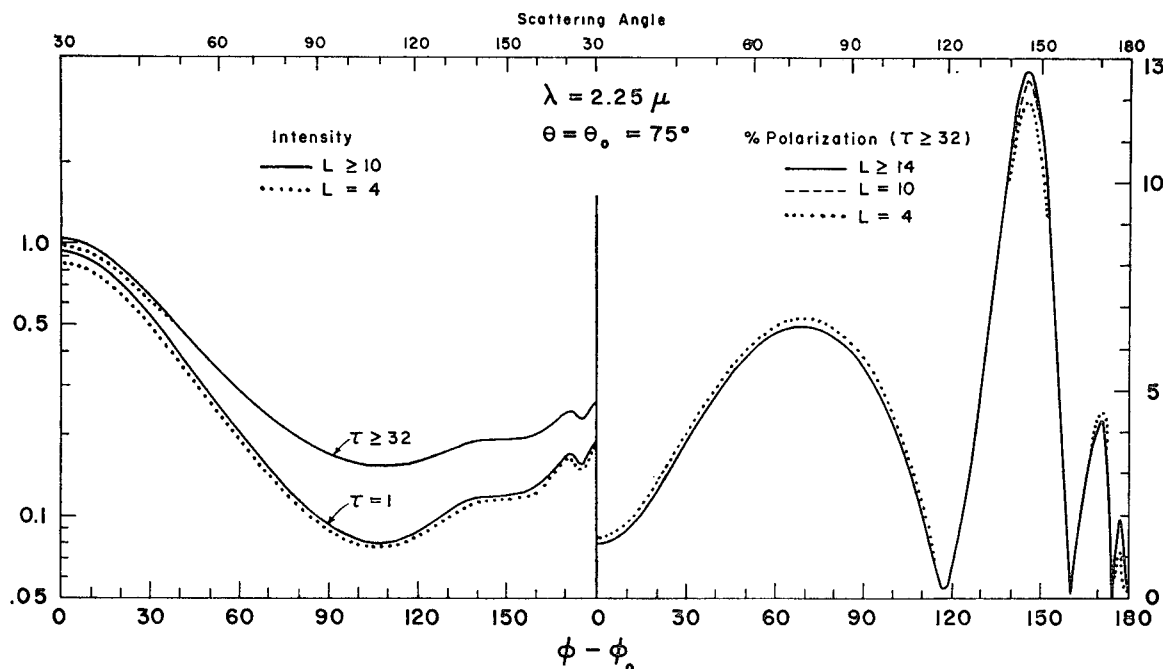


FIG. 26. Intensity ( $I = \mu_0 R^{11}$ ) and percent polarization  $[-100(Q^2 + U^2 + V^2)/I]$  of sunlight reflected by a plane parallel cloud for  $\theta = \theta_0 = 75^\circ$ .  $L$  is the order of the renormalization approximation, which is equal to the number of Gauss points used in the integrations over  $\mu$ . The wavelength is  $2.25 \mu$ . Two optical thicknesses are shown for the intensity and one for the polarization. The calculations are for the size distribution (1) with  $a = 6 \mu$  and  $b = \frac{1}{3}$ . In the percent polarization  $L = 10$  and  $L \geq 14$  are practically coincident except in the rainbow peak.

specified accuracy for reflected light. For a more anisotropic phase matrix the value of  $L$  required to obtain a specified accuracy is higher in both the discrete ordinate approximation and in the unmodified doubling method, and conversely the required value for  $L$  is smaller in both cases for more isotropic phase matrices.

If results are computed only for  $\mu$  and  $\mu_0$  equal to the Gauss points, then the computing time varies approximately as  $L^3$ . Thus, it is clear that the renormalization approximation can result in substantial savings in computation times. A disadvantage of the discrete ordinate method is that it often yields accurate results at such a small value of  $L$  that it is difficult to plot curves vs  $\mu$  or  $\mu_0$ . In that case results can be computed at extra zenith directions which are not used for evaluating the integrals over  $\mu$ . If  $L_x$  is the number of extra zenith directions, the computing time varies approximately as  $L(L + L_x)^2$ . Often a few well chosen extra zenith directions can serve to define sharp features in the reflected light.

The above form for the renormalization approximation was originally adopted specifically for the case in which polarization is neglected. It may well be possible to derive a still more accurate approximation for polarization, say by letting  $f_{ij}$  be different for different matrix elements, but we have not tried to do so. The above method was also adopted specifically for reflected light and it may be desirable to use a modified form if computations of the transmitted light are required.

## 6. Discussion

The computations presented in this paper are very encouraging on three counts. First it has been demonstrated that the theoretical approach is capable of handling the strongly anisotropic phase matrices which are typical of real cloud particles. In addition it has been found that characteristic features in the single scattering polarization survive the smoothing effect of multiple scattering, even for the thickest clouds; these features are hence potentially valuable for studies of cloud microstructure. Finally, several approximations in multiple scattering theory have been tested and shown to be useful for practical applications.

The most essential cloud characteristic which can be established by remote sensing is the phase of the cloud particles. In this paper we suggest that features which depend upon the spherical shape of water particles, particularly the primary rainbow, can be used for establishing the particle phase. We found that the polarization in the rainbow is typically several percent or higher, i.e., at least an order of magnitude greater than attainable observational accuracies. It is, of course, necessary to obtain more information about the polarization of light scattered by ice crystals, but it is safe to assume that features such as the rainbow, glory and supernumerary bows are absent for ice crystals, or at least greatly modified.

Calculations for multiple scattering may easily be made for ice spheres, but only certain characteristics of the resulting reflected light should be expected to represent real ice clouds. For thick clouds multiple scattering tends to wash out features in the phase function, so that the reflected intensity has little dependence on the particle shape. This indicates that the information content in the angular distribution of reflected intensities is limited, but it also means that it is reasonable to employ spherical particles in computations of spectral reflectivities. Hansen and Pollack (1970), for example, found that spectral reflectivities of terrestrial cirrus clouds could be matched quite well with calculations for a size distribution of spherical ice particles having a mean effective radius<sup>7</sup> of  $\sim 24 \mu$ . If the ice crystals are actually needle-shaped then this derived diameter of  $48 \mu$  should be larger than the needle diameter but much less than the needle length, because relatively few rays travel lengthwise through the needles.

However, spheres are less useful as an approximation for nonspheres when the polarization, rather than the intensity, is considered. This is a result of the facts that multiple scattering does not wash out features in the single-scattering polarization and that the single scattering polarization is sensitive to the particle shape. Diffracted light is similar for spheres and randomly oriented nonspherical particles, but it is unpolarized. For particles larger than the wavelength the only other rays expected to be closely similar for spheres and nonspheres are those externally reflected by the particles. In the limit of geometrical optics external reflection is the same for spheres and randomly oriented convex nonspherical particles (van de Hulst, 1957), and cirrus crystals should be close to the limit of geometrical optics (Liou and Hansen, 1971). Thus, at wavelengths where external reflection contributes heavily to the polarization, e.g., for  $\lambda \gtrsim 2.7 \mu$  in the near infrared, calculations for spherical ice particles are possibly useful. For example, Plass and Kattawar (1971) have recently shown that the polarization for ice spheres is larger than that for water spheres, because of the larger size of the ice particles. This fact could thus be useful at some wavelengths for particle phase determination, though the effect of possible ice crystal orientation must still be examined. Moreover, at wavelengths where the particles are essentially clear the polarization is dominated by rays which have traveled within the particle, and the polarization of such rays must differ significantly for spheres and real ice crystals. Theoretical computations for nonspherical particles are, of course, needed to help clarify the differences to be expected between spheres and nonspheres. At the present time an empirical study, involving extensive observations on clouds known to consist of ice

crystals, may be the most practical way to obtain more detailed knowledge of the polarization for ice clouds.

One application of the ability to establish the particle phase would be the detection of the phase change (water  $\rightarrow$  ice) which often precedes or accompanies the onset of precipitation from individual clouds and cloud systems. Such a detection by means of the polarization of reflected sunlight would become possible once the cross-sectional area of the ice crystals in the cloud top reaches a value on the same order as the cross-sectional area of the water particles in the same part of the clouds. Therefore, a detailed knowledge of the microphysical changes in the very tops of the clouds (where single scattered photons arise) is needed to assess the practicality and usefulness of detecting the phase change. An empirical study of the polarization of developing clouds is essential and should be made in conjunction with visual observations of the clouds and direct samplings of the cloud particles.

The computations in this paper illustrate that the polarization in the near infrared is sensitive to the particle size, as well as to the particle phase. The sensitivity to particle size is especially high in the  $3.0\text{--}3.5 \mu$  wavelength region. The interpretation of observed polarization is simplified in this region by the fact that practically all clouds are sufficiently thick for the polarization to be independent of the cloud optical thickness. The accuracy with which particle sizes can be estimated from polarization observations will therefore depend partly on the accuracy with which measurements can be made in the  $3.0\text{--}3.5 \mu$  region, where the observations may be hampered by the low solar flux and by thermal emission from the clouds and surroundings.

One application of particle sizing is the further discrimination of cloud type (in addition to the determination of particle phase). This application is complicated by the dependence of the cloud particle size distribution on various factors such as the nature of the cloud nuclei and by the problem of determining the best classification scheme for cloud studies and weather prediction. It is known, however, that there are correlations of the cloud particle size distribution and the meteorological conditions. For example, when a water cloud changes from a non-raining to a raining state, without going through the ice phase, both  $\langle r \rangle_{\text{eff}}$  and  $v_{\text{eff}}$  increase significantly. It is necessary that more information be obtained on the relation of the size distribution *in cloud tops* to the cloud type and to the development of clouds. It should be emphasized, however, that the fact that the polarization data refers to the cloud tops may be an advantage, because it would be difficult to interpret observations which refer to some average over the entire cloud depth.

The figures in this paper show the polarization and intensity as a function of angle, with the wavelength dependence only contained implicitly in intercompari-

<sup>7</sup> For the size distribution (1) with  $b = \frac{1}{2}$ , the mean effective radius is  $\frac{3}{2}$  times the mode radius.

sons of different figures. This presentation seems desirable as a first step because it is convenient for computations and clearly illustrates features, such as the rainbow and glory, and the effect of multiple scattering on these features. However, the variations in the polarization with wavelength, and particularly the fact that different wavelengths are sensitive to different cloud properties, point out the potential value of observations of the explicit wavelength dependence of the polarization. It has previously been found that the spectral dependence of the intensity is more sensitive than the angular dependence to cloud microstructure, and the value of observations of the wavelength dependence of the polarization has been emphasized by Gehrels and Teska (1963) and Coffeen and Gehrels (1969). For cloud studies such observations would provide the exciting possibility of a "snapshot" of polarization properties of a particular cloud area without the necessity of varying the scattering angle. Therefore, it would be worthwhile to extend the theoretical studies to include explicit illustrations of the wavelength dependence of the polarization.

*Acknowledgments.* I would like to thank D. L. Coffeen and J. W. Hovenier for useful discussions and comments on this paper. I am supported by NASA Grant 33-008-012 through Columbia University.

#### APPENDIX A

##### Characterization of the Size Distribution

In general, for the purpose of describing the scattering properties of a particle size distribution, a useful characteristic of the distribution is the *mean radius for scattering* (Hansen and Pollack, 1970)<sup>8</sup>

$$\langle r_{sc} \rangle = \frac{\int_0^\infty r \pi r^2 Q_{sc}(r, \lambda) n(r) dr}{\int_0^\infty \pi r^2 Q_{sc}(r, \lambda) n(r) dr}, \quad (A1)$$

where  $Q_{sc}(r, \lambda) \equiv Q_{sc}(x, n_r, n_i)$  is the efficiency factor for scattering (van de Hulst, 1957), and  $n_r$  and  $n_i$  are the real and imaginary parts of the particle refractive index. A particle of radius  $r$  scatters an amount of light in proportion to  $\pi r^2 Q_{sc}(r, \lambda)$  which explains the appearance of that weight factor in the definition of the mean radius for scattering. Similarly, we define the *relative variance for scattering* by

<sup>8</sup> Hansen and Pollack worked with the mean radius for extinction,  $\langle r \rangle_{ext}$ , because they were primarily concerned with the depth of spectral absorption features. For scattering by clouds in the visual and near infrared, however, there is little difference in the values of  $\langle r \rangle_{sc}$  and  $\langle r \rangle_{ext}$ .

$$v_{sc} = \frac{\int_0^\infty (r - \langle r \rangle_{sc})^2 \pi r^2 Q_{sc}(r, \lambda) n(r) dr}{\langle r \rangle_{sc}^2 \int_0^\infty \pi r^2 Q_{sc}(r, \lambda) n(r) dr}, \quad (A2)$$

where the factor  $\langle r \rangle_{sc}^2$  is included in the denominator to make  $v_{sc}$  dimensionless and a relative measure.

K. N. Liou and the author have made extensive computations (unpublished) with different size distributions having the same values for  $\langle r \rangle_{sc}$  and  $v_{sc}$ . These computations indicate that such size distributions have very similar scattering properties.

The appearance of  $Q_{sc}(r, \lambda)$  in (A1) and (A2) is inconvenient because it makes  $\langle r \rangle_{sc}$  and  $v_{sc}$  wavelength-dependent. However, since the ratio of the typical cloud particle size to the wavelength in the near infrared is at least on the order of unity, it is clear that the *mean effective radius* and the *effective variance*, defined by (2) and (3) in Section 2, will characterize the scattering properties of a cloud particle size distribution almost as well as  $\langle r \rangle_{sc}$  and  $v_{sc}$ . In the limit of very large particles  $\langle r \rangle_{sc} = \langle r \rangle_{eff}$  and  $v_{sc} = v_{eff}$ . It is, however, only necessary for  $\pi \langle r \rangle_{eff} (n_r - 1)$  to be  $\gtrsim \lambda$  in order for  $\langle r \rangle_{eff}$  and  $v_{eff}$  to be good parameters [see, e.g., Fig. 32 of van de Hulst (1957)], and this is valid for terrestrial clouds at near infrared and shorter wavelengths.

#### APPENDIX B

##### Derivation of $f_{ij}$

Let  $L$  be the order of the renormalization approximation, i.e., the number of Gauss points to be used for  $\mu$  on the interval (0,1), and  $w_i$  be the Gauss weight corresponding to  $\mu_i$ ,  $i=1, L$ . Also let

$$\begin{aligned} f_{ij}^1 &= 1, \\ r_j &= \sum_{i=1}^L {}^0P_r^{11}(\mu_i, \mu_j) w_i, \\ t_j^1 &= \sum_{i=1}^L {}^0P_t^{11}(\mu_i, \mu_j) w_i, \\ \epsilon_j^1 &= |1 - r_j - t_j^1|. \end{aligned}$$

If  $\epsilon_j^1 < 10^{-14}$  for all  $j=1, L$ , we take  $f_{ij} = f_{ij}^1$ ; otherwise, we compute successive estimates,  $f_{ij}^k (k=2, 3, \dots)$ ,

$$\begin{aligned} f_{ij}^k &= \frac{1}{2} f_{ij}^{k-1} \left( \frac{1-r_j}{t_j^{k-1}} \right) + \frac{1}{2} f_{ji}^{k-1} \left( \frac{1-r_i}{t_i^{k-1}} \right), \\ t_j^k &= \sum_{i=1}^L f_{ij}^k {}^0P_t^{11}(\mu_i, \mu_j) w_i, \\ \epsilon_j^k &= |1 - r_j - t_j^k|. \end{aligned}$$

The iterations are continued until for some  $k \equiv K$ ,  $\epsilon_j^K < 10^{-14}$  for all  $j=1, L$ . We then take  $f_{ij} = f_{ij}^K$ .

## REFERENCES

- Abhyankar, K. D., and A. L. Fymat, 1970: Imperfect Rayleigh scattering in a semi-infinite atmosphere. *Astron. Astrophys.*, **4**, 101–110.
- Allen, C. W., 1963: *Astrophysical Quantities*. London, Athlone, 291 pp.
- Blau, H. H., R. P. Espinola and E. C. Reifstein, 1966: Near infrared scattering by sunlit terrestrial clouds. *Appl. Opt.*, **5**, 555–564.
- Chandrasekhar, S., 1960: *Radiative Transfer*. New York, Dover, 393 pp.
- Coffeen, D. L., 1969: Wavelength dependence of polarization. XVI. Atmosphere of Venus. *Astron. J.*, **74**, 446–460.
- , and T. Gehrels, 1969: Wavelength dependence of polarization. XV. Observations of Venus. *Astron. J.*, **74**, 433–445.
- Dave, J. V., and J. Gazdag, 1970: A modified Fourier transform method for multiple scattering calculations in a plane-parallel Mie atmosphere. *Appl. Opt.*, **9**, 1457–1466.
- Deirmendjian, D., 1964: Scattering and polarization properties of water clouds and hazes in the visible and infrared. *Appl. Opt.*, **3**, 187–196.
- , 1969: *Electromagnetic Scattering on Spherical Polydispersions*. New York, Elsevier, 290 pp.
- Diem, M., 1948: Messungen der Grösse von Wolkenelementen II. *Meteor. Rund.*, **1**, 261–273.
- Durbin, W. G., 1959: Droplet sampling in cumulus clouds. *Tellus*, **11**, 205–215.
- Gehrels, T., and T. M. Teska, 1963: The wavelength dependence of polarization. *Appl. Opt.*, **2**, 67–77.
- Hansen, J. E., 1969a: Radiative transfer by doubling very thin layers. *Astrophys. J.*, **155**, 565–573.
- , 1969b: Exact and approximate solutions for multiple scattering by cloudy and hazy planetary atmospheres. *J. Atmos. Sci.*, **26**, 478–487.
- , 1970: Absorption-line formation in a scattering planetary atmosphere: A test of van de Hulst's similarity relations. *Astrophys. J.*, **158**, 337–349.
- , 1971: Multiple scattering of polarized light in planetary atmospheres. Part I. The doubling method. *J. Atmos. Sci.*, **28**, 120–125.
- , and J. W. Hovenier, 1971: The doubling method applied to the multiple scattering of polarized light. *J. Quant. Spectry. Radiative Transfer*, **11**, 809–812.
- , and J. B. Pollack, 1970: Near-infrared light scattering by terrestrial clouds. *J. Atmos. Sci.*, **27**, 265–281.
- Herman, B. J., 1965: Multiple scatter effects on the radar return from large hail. *J. Geophys. Res.*, **70**, 1215–1225.
- , and S. R. Browning, 1965: A numerical solution to the equation of radiative transfer. *J. Atmos. Sci.*, **22**, 559–566.
- , and R. J. Curran, 1971: The effect of atmospheric aerosols on scattered sunlight. *J. Atmos. Sci.*, **28**, 419–428.
- Holland, A. C., and G. Gagne, 1970: The scattering of polarized light by polydisperse systems of irregular particles. *Appl. Opt.*, **9**, 1113–1121.
- Hovenier, J. W., 1971: Multiple scattering of polarized light in planetary atmospheres. *Astron. Astrophys.*, **13**, 7–29.
- Hovis, W. A., and M. Tobin, 1967: Spectral measurements from 1.6  $\mu$  to 5.4  $\mu$  of natural surfaces and clouds. *Appl. Opt.*, **6**, 1399–1402.
- Hunt, G. E., 1971: The effect of course angular discretization on calculations of the radiation emerging from a model cloudy atmosphere. *J. Quant. Spectry. Radiative Transfer*, **11**, 309–321.
- Irvine, W. M., and J. B. Pollack, 1968: Infrared optical properties of water and ice spheres. *Icarus*, **8**, 324–360.
- Kattawar, G. W., and G. N. Plass, 1968: Radiance and polarization of multiple scattered light from haze and clouds. *Appl. Opt.*, **7**, 1519–1527.
- , and —, 1971: Radiance and polarization of light reflected from optically thick clouds. *Appl. Opt.*, **10**, 74–80.
- Kendall, M. G., and A. Stuart, 1963: *The Advanced Theory of Statistics*. New York, Hafner, 433 pp.
- Khrgian, A. Kh., 1961: *Cloud Physics*. Israel Program Scientific Translation, Jerusalem, 392 pp.
- , and I. P. Mazin, 1952: Some data on the microstructure of clouds. *Tr. Tsent. Aerolog. Observ.*, **7**, 56.
- , and —, 1956: Analysis of methods of characterization of distribution spectra of cloud droplets. *Tr. Tsent. Aerolog. Observ.*, **17**, 36.
- Liou, K. N., and J. E. Hansen, 1971: Intensity and polarization for single scattering by polydisperse spheres. A comparison of ray optics and Mie theory. *J. Atmos. Sci.*, **28**, 995–1004.
- Ludwig, F. L., and E. Robinson, 1971: Observations of aerosols and droplets in California stratus II. *Tellus*, **23**, 164–175.
- Lyot, B., 1929: Recherches sur la polarisation de la lumière des planètes et de quelques substances terrestres. *Ann. Obs. Paris (Meudon)*, **8**, 161 pp.
- Okita, T., 1961: Size distribution of large droplets in precipitating clouds. *Tellus*, **13**, 509–521.
- Plass, G. N., and G. W. Kattawar, 1971: Radiative transfer in water and ice clouds in the visible and infrared region. *Appl. Opt.*, **10**, 738–748.
- Potter, J. F., 1970: The delta function approximation in radiative transfer theory. *J. Atmos. Sci.*, **27**, 945–951.
- Sekera, Z., 1966: Reductions of the equations of radiative transfer for a plane-parallel planetary atmosphere. Parts I and II. Rand Corp., RM-4951-PR and RM-5056-PR, Santa Monica, Calif.
- Squires, P., 1958: The microstructure and colloidal stability of warm clouds. Part I: The relation between structure and stability. *Tellus*, **10**, 256–261.
- Twomey, S., H. Jacobowitz and H. B. Howell, 1966: Matrix methods for multiple scattering problems. *J. Atmos. Sci.*, **23**, 289–296.
- van de Hulst, H. C., 1949: *The Atmospheres of the Earth and Planets*. University of Chicago Press, 434 pp.
- , 1957: *Light Scattering by Small Particles*. New York, Wiley, 470 pp.
- , 1971: Multiple scattering in planetary atmospheres. *J. Quant. Spectry. Radiative Transfer*, **11**, 785–795.
- Warner, J., 1969: The microstructure of cumulus cloud. Part I. General features of the droplet spectrum. *J. Atmos. Sci.*, **26**, 1049–1059.
- Weickmann, H. K., and H. J. aufm Kampe, 1953: Physical properties of cumulus clouds. *J. Meteor.*, **10**, 204–211.
- Zaitsev, V. A., 1950: Liquid water content and distribution of drops in cumulus clouds. *Tr. Gl. Geofiz. Observ.*, **19**, 122–132.